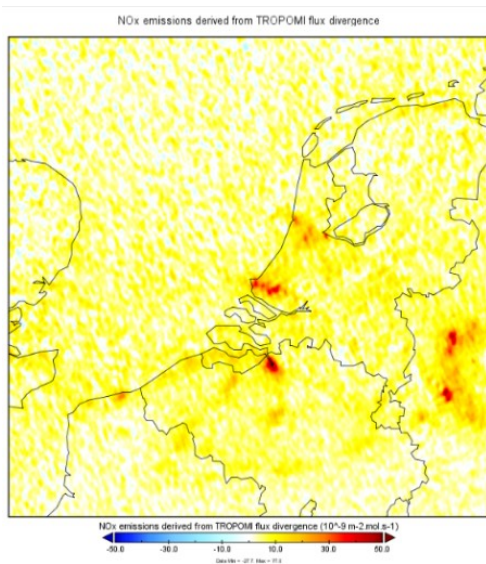


Determining emissions from NO₂ acquired from Sentinel-5P's TROPOMI.

ABSTRACT



In this study it will be investigated how emissions can be derived directly from TROPOMI NO₂ column observations and wind information. The area of interest will be the Netherlands and its neighbouring countries as well as Riyadh, Saudi Arabia. A divergence method is used to derive emissions of NO_x from NO₂ concentrations (TROPOMI) and wind data (ECMWF). This divergence method is able to estimate the emission of NO_x derived from TROPOMI for the Netherlands for different time periods. This was applied for the Netherlands for different time periods: one day, one week and one season. A comparison with TROPOMI emission estimates was made between EmisRegistatie (qualitatively) and CAMS emission estimates (quantitatively). To conclude, this divergence method is able to determine emission estimates spatially and quantitatively for different time periods, however this depends on location whether or not these emission estimates are of high quality.

AUTOR – N.S. Berkhout

FACULTY/DEPARTMENT – ITC – Water Resources

DATE: 22 June 2020

ADVISOR:

EXTERNAL SUPERVISOR – dr. H. Eskes (KNMI)

EVALUATION ASSESSMENT BOARD:

CHAIR - dr.ir. C.M.M. Mannaerts

FIRST SUPERVISOR - dr.ir. C. van der Tol

SECOND SUPERVISOR - dr. B.H.P. Maathuis

CONTENTS

Contents.....	2
1. introduction Societal & Research problem.....	4
1.1 Societal problem	4
1.2 Research problem	5
Sentinel-5P.....	6
2. Research questions.....	7
2.1 Interpretation of emissions from NO2 concentrations.....	7
2.2 Application of the method on Sentinel-5P's data and ECMWF's data.....	7
2.3 Analysis of emission estimates.....	7
3. Conceptual framework and related work.....	8
Earth's atmosphere.....	8
Impacts of tropospheric ozone	8
Warming and cooling effect of GHG's	8
Nitrogen oxides.....	9
methods for emission determination	10
3.1 Description of the Beirle method.....	11
Equations	11
1D model of the principles used in Beirle et al. (2019a; 2019b).....	13
4. Research design	15
4.1 study areas	15
4.2 Data.....	15
NO2 concentrations.....	16
Wind data.....	16
Data pre-processing.....	17

5.	method.....	18
5.1	Interpretation of emissions from NO ₂ concentrations in the Netherlands.....	18
5.2	Application of the method on Sentinel-5P's data and ECMWF's data.....	18
5.3	Analysis of emission estimates.....	20
6.	Results.....	21
6.1	Interpretation of emissions from NO ₂ concentrations in the Netherlands.....	21
6.2	Application of the method on Sentinel-5P's data and ECMWF's data.....	23
	importance Planetary boundary Layer	24
	Wind changes in the vertical column.....	25
6.3	Analysis of emission estimates.....	30
7.	Discussion	36
8.	conclusion & future recommendations.....	39
8.1	Future recommendations	39
9.	References	41

1. INTRODUCTION SOCIETAL & RESEARCH PROBLEM

For the Netherlands, the year 2019 begins with the Raad van State (highest administrative body) revoking the PAS policy, since it did not coincide with the European law for protection of nature. Since this revocation, there is an ongoing societal, economic and political discussion about how and why the Netherlands should change its policies regarding pasture farmland as NH₃, industry and air-, sea- and land- transportation as NO_x. These sectors have a negative impact on nature preservation, human health and the environment (TNO, 2019; WHO, 2003, 2005, 2016; Xie et al., 2019).

This problem started with the revocation of the PAS (Plan Aanpak Stikstof). In 2015, in the Netherlands, the government has created the PAS policy. This policy was set to reduce the reactive Nitrogen in the soil and in the atmosphere. Entrepreneurs and companies that were in farming, construction and industry and needed a permit to build or expand. They needed to compensate reactive Nitrogen during the construction of the project or with the project itself. Due to its contradiction with European Law, the Raad van State (highest administrative body) revoked the PAS policy.

1.1 Societal problem

Ammonia has an impact on ground water and soil. NO_x, on the other hand, is different since it reacts easily with other particles in the atmosphere and is often associated with human health problems (WHO, 2003, 2005, 2016; Xie et al., 2019). In order for NO_x to have an impact on the environment, it must first deposit. There are two types of deposition: dry and wet. Dry deposition is direct absorption of nitrogen compounds by vegetation and soil, whereas wet deposition is caused by precipitation (TNO, 2019). The depositions of nitrogen can change the species diversity, reduce richness and abundance of plant and animal species and it can even create a loss of special species (Dentener et al., 2006; Stevens et al., 2010; Xiankai, Jiang Ming, & Shaofeng, 2008). Nitrogenoxides (NO_x=NO + NO₂) are also called reactive Nitrogen (Nr) and do not only cause fine particles, add to the greenhouse gases, ozone and pollutes water but it also acidifies the soil, create a monoculture among plants, insects and animals and damages human health.

The majority of nitrogen affecting nature and the environment is caused by pasture farming as NH₃, the rest is caused by transportation, industry and domestic use as NO_x (TNO, 2019). This Nitrogen discussion has a two main components: Ammonia (NH₃) and Nitrogen oxides (NO_x). Even though, European Law has a set of rules for NO_x due to it affecting air pollution and human health, the discussion in the Netherlands focuses more on ammonia NH₃ than on NO_x. Due to the fact that pasture farming is the largest contributor, the discussion about Nitrogen has shifted its focus to pasture farming and the policies around it. This has caused that the general public and the media have neglected the impact of NO_x completely. That is a very unfortunate matter, since, there is still a lot to learn about NO_x.

Furthermore the time it takes for NO_x to react with other substances such as OH and aerosols varies per season due to the temperature (TNO, 2019; van Geffen, Eskes, Boersma, Maasakkers, & Veefkind, 2019). The extent that NO_x deposits near or far from the source is still on debate and is surrounded with uncertainty. According to TNO (2019) only a small amount of NO_x deposits and 90% of Dutch produced NO_x crosses the borders towards neighbouring countries. Also according to van Geffen et al. (2019), the NO₂ has a lifetime of several hours and stays close to its source. Both sources are in agreement that NO₂ can travel distances, conversely, how far NO₂ can travel within a time frame is still unclear.

1.2 Research problem

In this subsection, the advantages of Satellite imagery over AQ stations and the advantages of mathematical models over interpolation models will be explained.

Currently, in the Netherlands Air Quality stations (AQ stations) and models are used to determine concentration all over the Netherlands. The measurements by the "Landelijk Meetnet Luchtkwaliteit" (LML) of the RIVM form the backbone of this network, complemented by measurements of the GGD of Amsterdam and DCMR in Rotterdam. The data of the AQ stations are acquired over the whole Netherlands. The use of Air Quality stations, s measured at a limited number of locations in the Netherlands. And therefore, this system fails to derive depositions and emissions. Values of depositions and emissions within a certain scale are the crux of the matter in the discussion about the effects of NO₂ in the environment and human health. The AQ stations are used for calibrating and testing the models.

In the Netherlands, three different kinds of models are actively used for determining the concentration values for nitrogen dry and wet deposition (TNO, 2019). The first model is the OPS used by the Rijksinstituut voor Volksgezondheid en Milieu (RIVM, English: National Institute for Public Health and the Environment) for their Grootchalige Concentratie en Depositiekaarten Nederland (GCN/GDN, English: concentration and deposition maps for the Netherlands) (Velders et al., 2018). This model can calculate the deposition of NO_x using the wind direction, mixing altitude and transport distance (Sauter et al., 2018). Second model is the EMEP from the Meteorological Institute Norway and is often used to support policies on a European level (Klein, Gauss, Nyiri, & Benedictow, 2018). The third model is LOTOS-EUROS from Nederlandse Organisatie voor Toegepast Natuurwetenschappelijk Onderzoek (TNO, English: Netherlands Organisation for Applied Scientific Research). The Dutch LOTOS-EUROS model is used for daily air-quality forecasts for Europe (through the CAMS project) and the Netherlands (Manders et al., 2017). These forecasts are produced at KNMI and are disseminated to the Dutch public by RIVM. All models use national and European emission inventories to calculate the concentrations.

TNO (2019) compared the import and export of NO_x and NH₃ together in these models and found disagreement among the models. For any of the models it is difficult to measure the concentrations of NO_x, since wind, emissions and deposition influence the concentration of NO_x in the atmosphere. Unfortunately, emissions are never

determined using a model since they are used for the determination of concentration of the NO₂ as input in a model. Furthermore this difficulty is even more extended due to the limitation in AQ stations that measure NO_x, seven stations measure hourly averages for long time series, and ten stations can measure wet deposition (TNO, 2019). The choice of model determines the outcome of the depositions and emissions. Therefore it is difficult to say which model is the most accurate. The AQ stations are unevenly distributed and have a limited number to have a maximum coverage for the entire country. According to Mijling, Van Der A, & Zhang (2013) the inventories used are often not complete or outdated, whereas satellite imagery has consistency throughout space and have a good temporal resolution as well. For determining concentrations over the Netherlands, satellite imagery is a fast, cost-friendly and user-friendly tool to acquire the data.

SENTINEL-5P

Satellite measurements of NO_x can bridge the shortcomings of AQ stations. Since 2017, ESA has launched within its Copernicus Program a new satellite, Sentinel-5P, for atmospheric monitoring. This satellite has a new sensor, TROPOMI, which can measure ozone, nitrogen dioxide (NO₂), sulphur dioxide (SO₂), aerosols, carbon monoxide (CO), methane (CH₄) and clouds with a resolution of 7x3.5 km every day.

According to Williams et al. (2017), a transport model can be used to derive vertical profile of nitrogen dioxide (NO₂), sulphur dioxide (SO₂) and formaldehyde (CH₂O). Which in turn can be used for satellite retrievals from OMI, Sentinel-5P. Boersma et al. (2018)'s aim was to create a 22-year long record of the NO₂ column that crossed decades and was harmonious.

Sentinel-5P can help understand the processes of transport of NO_x and give insight to what degree the export and import of NO_x emissions and deposition are contributing to the total amount of NO_x concentrations in the air. This is especially interesting for the Netherlands, a net emitter (TNO, 2019). Sentinel-5P and other satellites on their own cannot fully answer the questions at hand about air pollution. In order to answer where sources of pollutants are, emission sources need to be estimated. A new method to calculate the emissions of NO₂ has been published last November 2019. The article by Beirle et al. (2019), describes how the emissions of NO_x can be determined using fluxes and divergences of measured concentration. Further explanation of this method can be found in *Chapter 3* as well as related work for emission estimation.

To help policy makers make decisions concerning reducing NO_x emissions, it is important to measure and to map both the NO₂ concentrations and the NO_x emissions. This study's aim is to determine emissions of NO_x using Sentinel-5P data of NO₂ concentrations and a divergence method (Beirle et al., 2019a) to calculate the emission sources of NO_x in the Netherlands and Riyadh, Saudi Arabia.

2. RESEARCH QUESTIONS

In this study it will be investigated how emissions can be derived directly from TROPOMI NO₂ column observations and wind information. If these emissions are realistic and statistically significant (relatively less noise). The method introduced in Beirle et al. (2019a) has been independently implemented at KNMI, and the software was used to derive emission maps for different time-averaging periods. The Research Questions are identified below.

2.1 Interpretation of emissions from NO₂ concentrations

- RQ 1 - Is it possible to identify the known emission sources using the total NO₂ tropospheric column measurements?

2.2 Application of the method on Sentinel-5P's data and ECMWF's data

- RQ 2 – Does our independent implementation of the method reproduce the results presented in Beirle et al. (2019)?
- RQ 3 – What is the optimal height for the wind to be used to determining emissions for the Netherlands and elsewhere?

2.3 Analysis of emission estimates

- RQ 4 – What is the minimal integration time that can be used to obtain a useful map for emission estimates?
 - Which regions are more suitable for the method of Beirle?
- RQ 5 – How does the method of Beirle compare to independent emission estimates for the Netherlands?

3. CONCEPTUAL FRAMEWORK AND RELATED WORK

EARTH'S ATMOSPHERE

The Earth's atmosphere mainly consists of three main gases: nitrogen (N₂), oxygen (O₂) and argon (Ar). These gases are present in the air at nearly constant mixing ratios everywhere in the atmosphere, due to their long residence time (Berner & Berner, 2012). However air consists of a mixture of trace gases with small mixing ratios measured in parts per million, billion or even per trillion. Despite these small concentrations, these trace gases and particles play a crucial role and determine the heat balance in global warming and responsible for air pollution. The ratio between these gases can be influenced by natural and human processes (Berner & Berner, 2012). Gases that have increased due to anthropogenic activities are: carbon dioxide (CO₂), methane (CH₄), nitrous oxide (N₂O), ammonia (NH₃), ozone (O₃), carbon monoxide (CO), sulphur dioxide (SO₂) and nitrogen oxides (a combination of NO₂ and NO represented as NO_x).

IMPACTS OF TROPOSPHERIC OZONE

Tropospheric ozone is a gas that affects human, animals and plants and at the same time is caused by anthropogenic activities (Ahmed Bhuiyan, Rashid Khan, Zaman, & Hishan, 2018; Berner & Berner, 2012). According to Forster (2007) tropospheric ozone is after carbon dioxide and methane the most important greenhouse gas. Tropospheric ozone is a product of nitrogen oxides, methane, carbon monoxide and nonmethane volatile organic carbon compounds. Which means that, transportation, industry, biomass burning and burning of fossil fuels, results in an increase in methane (CH₄), carbon monoxide (CO) and nonmethane volatile organic carbon compounds (NMVOCs) and nitrogen oxides (NO_x) (Berner & Berner, 2012; Dentener et al., 2006; Stevenson et al., 2006). Ozone in the troposphere is a pollutant that affects humans, animals and plants and is caused by the mix of hydrocarbons and nitrogen oxides in the form of transportation and industry (Berner & Berner, 2012; Dentener et al., 2006; Stevenson et al., 2006).

WARMING AND COOLING EFFECT OF GHG'S

Looking at the effect these gases have on climate, biodiversity and human health it is clear there are distinct differences between these gases. On one hand we have major greenhouse gases such as CO₂, CH₄ and N₂O and minor greenhouse gases such as tropospheric ozone (O₃) and nitrogen oxides (NO_x) on the other hand (Paolini et al., 2018; Yasmeen, Li, & Hafeez, 2019). Carbon dioxide and methane both have a warming effect on the global climate (Paolini et al., 2018; Yasmeen et al., 2019). The major greenhouse gases have a warming effect on the global climate, for the minor, especially NO_x this is slightly complicated. Nitrogen oxides are more reactive than CO₂ and CH₄ and causes nitrate formation. This nitrate formation causes an increase in aerosol concentrations

(van Geffen et al., 2019). These aerosol concentrations have cooling effect on the climate. Therefore, nitrogen oxides have a net cooling effect on the global climate even though it is a minor greenhouse gas (van Geffen et al., 2019). In short, nitrogen oxides have a warming and a cooling effect on the earth's climate depending on where nitrogen oxides are in the atmosphere.

NITROGEN OXIDES

The presence of NO_x in the vertical column is crucial for the consequences NO_x has on the environment, ozone layer and human health. In the troposphere, nitrogen dioxide (NO₂) reaction with OH results in tropospheric ozone whereas in this same tropospheric layer, NO₂ reacts with oxidants, form nitrate formation which in turn results in aerosols and therefore a decrease in temperature of the atmosphere (Shindell et al., 2009). For the stratosphere, the effect of NO₂ is slightly different. NO₂ is caused by N₂O oxidants in the middle stratosphere and indirectly causes a depletion of the ozone layer through a photochemical process (van Geffen et al., 2019).

Nitrogen oxide (NO_x) has a severe impact on the global climate. The lifetime of NO_x is only several hours, it can range from 4 to 8 hours depending on the latitude, altitude and season. Meaning that NO_x can travel greater distances in the winter due to the fact that the lifetime of NO_x in the winter is longer than it is in the summer, but overall, NO_x stays within 100 km to the source (van Geffen et al., 2019). According to TNO 2019, NO_x as a gas cannot travel great distances. However NO_x can travel far and beyond borders when it reacts with the atmosphere and results in small fine particles that include nitrogen (TNO, 2019; van Geffen et al., 2019). The NO_x in this part of the atmosphere stays close to the source with its short lifetime and causes implications for human health, specifically respiratory problems (Berner & Berner, 2012; Shindell et al., 2009; van Geffen et al., 2019). This type of NO_x can when deposited ignite the process of eutrophication (Dentener et al., 2006).

The most common air pollutants are tropospheric ozone and NO_x (Ahmed Bhuiyan et al., 2018). In recent years an increase in potentially dangerous gases have been monitored. on a global level between 1970s-1980s there was a rapid increase in concentrations of tropospheric ozone, however between 1990s-2010 especially in the Northern hemisphere only on a regional level there was a change in tropospheric ozone (Oltmans et al., 2013). Nitrogen oxides and Ammonia are a great contributor to the tropospheric ozone increase and to a change in biodiversity in near-by nature areas (Ahmed Bhuiyan et al., 2018). According to TNO (2019), 60% of nitrogen deposits as NH₃. Nitrogen oxides (NO_x) are mainly produced by transport sector and the industry whereas ammonia (NH₃) is often produced by husbandry farming due to manure injecting (TNO, 2019).

Sentinel-5P is the satellite where TROPOMI is the sensor that carries out the measurements of NO₂ concentrations. TROPOMI measures radiance with its high spectral resolution and NO_x is a product derived from

these measurements. Due to the short lifetime of NO₂ in the air, TROPOMI can measure the NO₂ easily. And NO₂ can travel long distances which makes pin-pointing the source of that concentration easier than for CO₂. However, the resolution of Sentinel-5P is not suitable yet for emissions but only for concentrations. Concentrations of NO₂ and their derived emissions give a complete package of information. Whereas emission is influenced by internal factors such as the source, concentration is also affected by external factors such as wind and precipitation (Ding, Van Der A, Mijling, Levelt, & Hao, 2015). Since travel distances of NO₂ are depending on wind directions and speed, a divergence method can be used to calculate the emissions from the position of the concentration and wind information.

METHODS FOR EMISSION DETERMINATION

There have been other publications that derive emissions from pollutant's concentrations. Jury (2017) and Tanzer, Malings, Haurlyliuk, Subramanian, & Presto (2019) both use in situ measurements for the emissions. Jury (2017) uses satellite data such as Ozone Monitoring Instrument (OMI) and Atmospheric Infrared Sounder (AIRS) and derive CO₂, SO₂ and NO_x **emissions**, whereas Tanzer et al. (2019) uses statistics and known concentration measurements and derive emissions for SO₂ and NO₂.

In Lorente et al. (2019), the aim of the study is to estimate the NO_x emissions from Paris directly from TROPOMI NO₂ columns using a method that does not need a complex chemistry transport model. In this study, the TROPOMI NO₂ columns are validated against AirParif in situ NO₂ concentration measurements. Not only satellite data is used but also wind speeds. In Lorente et al. (2019), emission are estimated using concentrations within the boundary of the city rather than plumes outside the city of Paris. The lifetime of NO₂ in the boundary level is not of importance since it crosses the Paris centre relatively fast in comparison to how much time it cost to decay the chemical compound completely. Eventually, the study compared the NO_x emissions to two inventories instead of using a derivative for the emissions.

In Goldberg et al. (2019), a reprocessing of the vertical column of NO₂ (TROPOMI) was done using an air mass factor. Afterwards the derived emission rates for NO_x was compared to projected bottom-up emission inventories. Also, the sub-seasonal variability of NO_x emissions was assessed by using a single season (Goldberg et al., 2019).

Another method that is used for emission determination is the Daily Emission estimates Constrained by Satellite Observations (DECSO) algorithm (Mijling & Van Der A, 2012). This algorithm uses an ensemble Kalman filter to compute emissions. It uses an inversion for daily assimilation as well as taking into account the local and non-local concentrations. DECSO combines simulated regional Chemistry Transport Model (CTM)'s NO₂ concentrations with

observed satellite imagery (Ding et al., 2018). DECSO is an inversion-based algorithm that is often used in computing emissions for NO_x (Ding et al., 2018; Mijling & Van Der A, 2012).

In this study an alternative approach to derive emissions, introduced by Beirle et al. (2019a). In Beirle et al. (2019a), emissions of NO₂ are determined from the tropospheric column of TROPOMI by calculating fluxes from the wind and concentrations of NO₂. A gradient was applied to the flux to calculate the divergence. The concentration is divided by the lifetime and this results in sinks. These sinks are added to the divergence to create emission estimates. This is because sinks are convergence of fluxes and divergence is source of fluxes. Therefore sinks are also used in the estimation of emissions.

3.1 Description of the Beirle method

In (Beirle et al., 2019a, 2019b) a divergence method concerning wind data and NO₂ is used to derive emissions from concentrations. Fluxes were derived from concentrations and winds while divergence was derived using numerical derivatives from the fluxes. Sinks were calculated using concentrations divided by lifetime. This method uses sinks (convergence) and divergence together to calculate the emissions. The reason for using the Beirle method over the previously mentioned is because it can be used without determining plumes first and this method can be applied directly on TROPOMI's data. In the next subsection, this method mentioned in Beirle et al. (2019) is explained in more detail.

EQUATIONS

Generally, a source (emitter) emits a substance, this concentration is transported by wind over an area. This area (plume) can be seen using satellite data. Thus, emission causes an increase in concentration at the source, this increase is calculated using the divergence. The Beirle method (Beirle et al., 2019a) can briefly be explained using equations. Wind passes over a source and transports the emitted concentration of NO₂, the location of the source can be derived when observing the direction of the wind, speed of the wind and the lifetime.

In the equations below (eq. 3.1 & 3.2), adapted from Beirle et al. (2019a), L is used as the ratio of NO_x / NO₂ and is used in converting NO₂ concentrations to NO_x emissions. The NO₂ concentration called V [mol m⁻²] is multiplied with wind raster data, w , [m s⁻¹] to calculate the flux, Vw , [mol m⁻² s⁻¹] in x- and y-direction. A spatial derivative is applied to the flux to calculate the divergence D [mol m⁻² s⁻¹]. Sinks of NO_x [mol m⁻² s⁻¹] are described as LW/τ where τ is the lifetime of NO_x in seconds and chosen by Beirle et al. (2019a) as a fixed value $4 \cdot 3600$ [s]. Afterwards divergence is added to the sinks to result in emissions [mol m⁻² s⁻¹].

$$D = E - S \quad \text{eq. 3.1}$$

$$S = \frac{V}{\tau}$$

$$D = \nabla LV_w$$

$$E = L \frac{V}{\tau} + \nabla LV_w \quad \text{eq. 3.2}$$

Further details regarding the equations and its use in emission determination is explained in *Chapter 0*. In the next subsection, a 1D-model is used to explain how the method works.

1D MODEL OF THE PRINCIPLES USED IN BEIRLE ET AL. (2019A; 2019B)

This 1D model is visualised in four different graphs. All graphs represent concentration [mol] (black), flux [mol km h⁻¹] (green) and divergence [mol/h] (blue).

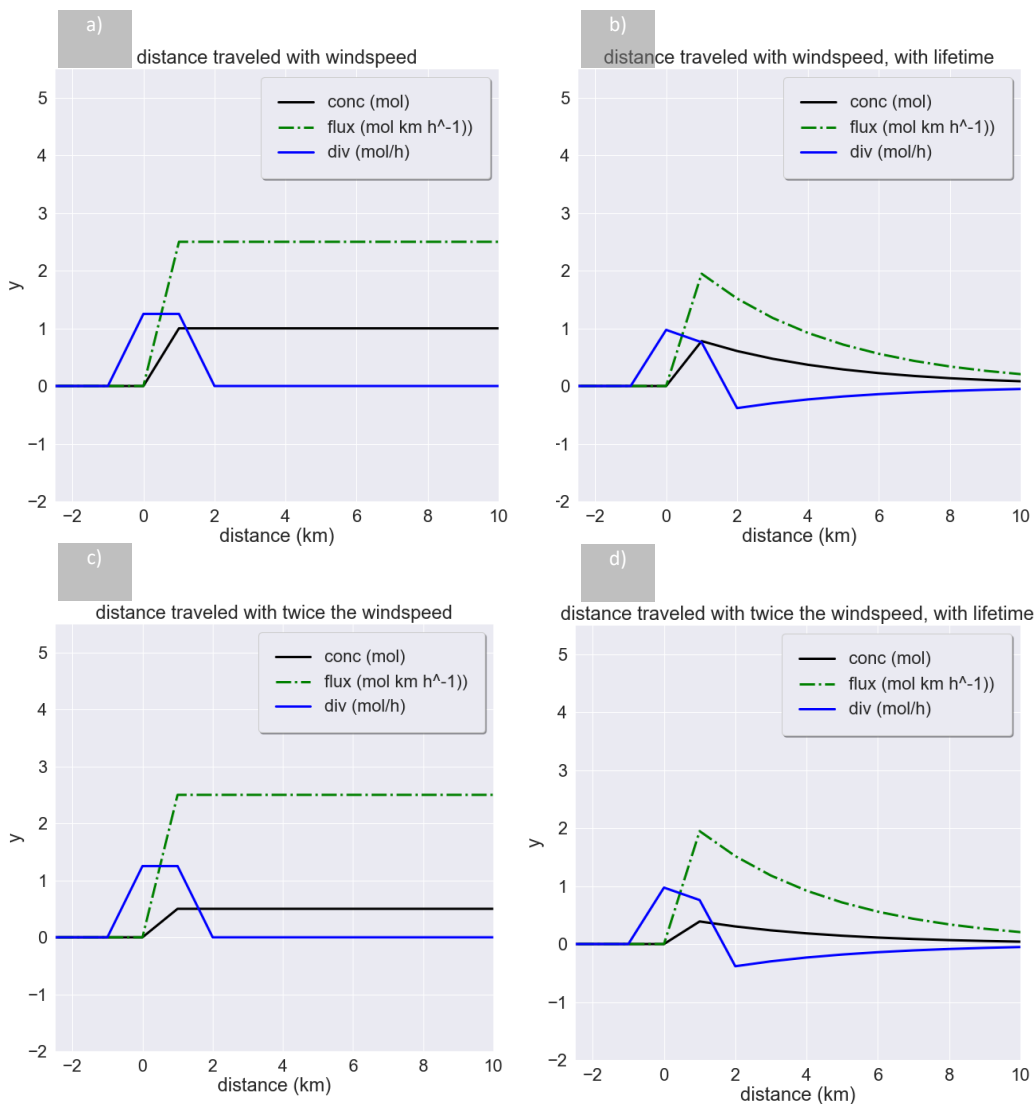


Figure 3-1 - 1D model of concentration, flux and divergence without lifetime (left) and with lifetime (right). And with windspeed of 2.5km/h (top) and 5km/h (bottom)

Many sources, such as a power plant, will behave as a continuous emission source with a constant emission of NO_x per hour. Figure 3-1a shows the behaviour of one plume (concentration) that is created by this emission source and transported by a constant wind speed of 2.5 km/h. The pre-defined emission is added to the concentration with each timestep. This block of concentration moves along the x-axis to the right. Therefore, throughout time and therefore space, the concentration is constant throughout the plume. All graphs use distance in [km] on the x-axis, concentration and therefore divergence are related to the windspeed. For Figure 3-1a and Figure 3-1b, the windspeed is 2.5 [km h⁻¹], the starting concentration is 0 [mol h⁻¹] with emission of 1.0 [mol h⁻¹] added for every timestep and the timestep is 1 [km⁻¹]. Figure 3-1b (and Figure 3-1d) has a lifetime of NO_x in its graph. Lifetime in these graphs is an exponential decay and decreases according to concentration. The graph without lifetime (Figure 3-1a & 3-1c) depicts how emissions and concentrations act throughout one dimensional space and the graph with lifetime depicts how these change over the distance [km].

In Figure 3-1c and Figure 3-1d the windspeed is twice as in Figure 3-1a and Figure 3-1b, it is 5 [km h⁻¹]. These figures have the same starting concentration value and the same timestep as in Figure 3-1a and Figure 3-1b. With increasing wind speed, the concentration decreases while flux and divergence stay the same (Figure 3-1c and Figure 3-1d). Divergence has near the source (at distance = 1km) decreasing negative values (sinks) because concentration is decaying due to the lifetime and is declining in its spread over distance (Figure 3-1b and Figure 3-1d). This concurs with the fact that emission is divergence and these sinks (deposition and chemical reaction) added together. Since the integral of the divergence is zero, the emission will decrease with distance towards zero. Eventually with distance, concentration will be reduced to zero as well (Figure 3-1b and Figure 3-1d).

4. RESEARCH DESIGN

4.1 study areas

In this study, the area of interest will be the Netherlands and its neighbouring countries as well as Riyadh, Saudi Arabia. The Netherlands has multiple sources of emission data (such as EmissieRegistratie.nl and the Copernicus Atmospheric Monitoring Service (CAMS) from TNO). Riyadh, on the other hand, will be used as an example for the method applied in Beirle et al. (2019a).

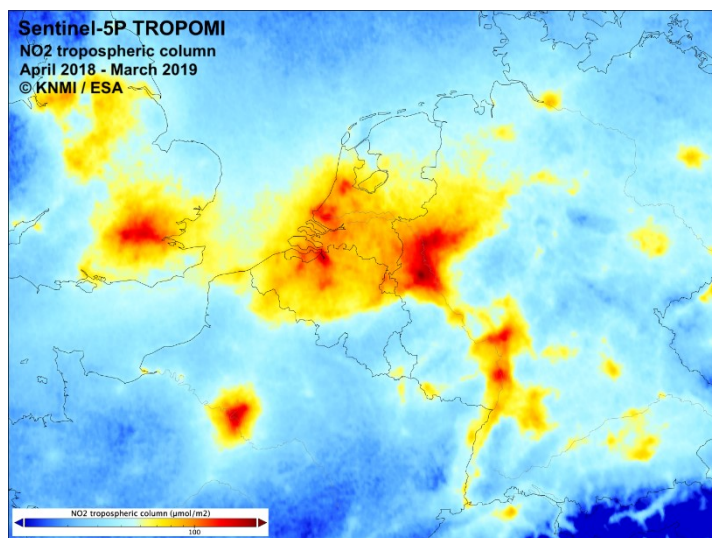


Figure 4-1 - Aggregated image of No₂ concentrations above Northern Europe for the time period of April 2018 - March 2019. with a resolution of 2x2km

In this study, the emphasis will be on industry and transport for NO_x. On the left (Figure 4-1), an aggregated image of NO₂ by Sentinel-5P from April 2018 – March 2019 with a resolution of 2x2km is shown. This image shows clearly that big cities (such as London, Antwerp, Paris) and industrious areas (such as Schiphol Airport, Rotterdam Harbour and Ruhr industrious area) have high amounts of NO₂ concentrations above them.

According to Van Geffen et al. (2019), the spatial resolution of Sentinel-5P's TROPOMI is 7x3.5km. This limitation inhibits the possibility to analyse transport in the Netherlands, however large scale concentrations due to

industry is possible. However this study will emphasise on the Netherlands. Due to the scope of the study area and the absence of a relation between air pollution and borders, NO₂ plumes in the vicinity of the Netherlands will also be taken into account.

4.2 Data

The data used in this study are NO₂ concentration raster data and wind raster data at multiple altitudes, required at the Copernicus Hub and from ECMWF's operational data through the KNMI respectively. Both are data for the three time periods: one day (28th June 2019), one week (23rd – 29th June 2019) and three months (June, July and August 2019). These periods were chosen based on minimal cloud coverage above the Netherlands.

NO₂ CONCENTRATIONS

For the NO₂ data, satellite imagery of Sentinel-5P is used, specifically from TROPOMI sensor. The data of Sentinel-5P are offline and level 2 datasets. Level 2 data imagery has got geolocated total column of nitrogen dioxide whereas Level 1 only has measurements of solar irradiances and all spectral bands. Near Real Time datasets of Sentinel-5P are used as a processing type, because it is within 3 hours available after sensing. However, offline datasets are datasets older than 2 months and can be used as reprocessed datasets that are checked and ready for analysis. For the time period of June – August 2019 (one season) the offline (reprocessed) data of Sentinel-5P is used. The datasets are NetCDF4 files and have different variables within the NetCDF4 file. These variables are subdatasets such as nitrogen dioxide total column, quality flags, latitude and longitude.

Even though the time period chosen has got a minimal cloud coverage, for whole of North Europe or even larger regions, cloudy pixels are present. Quality flag-values from the ATBD (van Geffen et al., 2019), 0.75-1.00 have been used to filter out all pixels that are of low quality, meaning that the cloudy pixels are removed as well from the image. The pixels who did not have a quality flag of above 75% (0.75) were removed using Python 3.7 (Appendix 1-script).

In the ATBD document and in the PUM (Product User Manual) quality flags are described that can be used to differentiate between clear-sky pixels, clouds, snow and ice (Eskes et al., 2019; van Geffen et al., 2019). Two different quality flags existed in the PUM (Product User Manual) document for the Sentinel-5P's data (Eskes et al., 2019). The quality flags (QF) ranged from 0.00-1.00 and two distinctive quality flags were used, 1) QF 0.50 – 1.00 and 2) QF of 0.75 – 1.00. Both remove errors and problematic retrievals however QF of 0.50 shows pixels with clouds over snow-covered areas whereas a QF of 0.75 or higher removes all pixels with clouds and snow/ice. Unfortunately, some orbits had clouds in the imagery, which had to be removed using the second QF of 0.75 and higher. Pixels that did not meet the QF of 0.75 and higher were set as undefined in the orbits visual representation. A new image including the quality flags was reproduced for later analysing using Python 3.7.

WIND DATA

The operational wind data from the ECMWF is the most complete dataset for gridded meteorological data that exists at this moment. This dataset has a global resolution of 30 km grid cells and is available on single levels, pressure levels, potential temperature levels and model levels. This study uses the data on model levels.

Model levels means that the data uses model heights instead of pressure heights. Pressure levels depend on the temperature and density for converting to altitude, whereas model levels do not. model levels follows the height of the surface and model levels are independent from temperature. Especially for comparing wind data of different seasons and using wind data over mountainous areas, using model levels is easier to convert and to calculate with.

The wind dataset is a NetCDF3-classic file format. In the wind raster data files, it has two datasets: U and V components. These are the directions in x and y and can be combined to get the speed and direction of the wind. Furthermore these wind files consists of each level (107-137) and hours (00-24h) consisting of 31x24=744 layers for each day. Since the NO₂ concentrations are measured around 12h above the Netherlands, 12h00 UTC was chosen for these wind data files as well.

DATA PRE-PROCESSING

Furthermore the resolution of the pixels were regrided from 7x3.5km (Sentinel-5P) to 2x2km and from 30x30km (ECMWF) to 2x2km. This was done by KNMI. There are two reasons for regriding: 1) the pixels do not give the impression that it is stretched (rectangular pixels) but they become square, 2) for estimating emission, a 2x2km grid allows itself for better estimates than 7x3.5km. The method behind this regriding involves weights. In essence, the pixel is divided in smaller grids of 2x2km, the area that overlaps the part of the pixel into the 2x2km grid cell is filled with the value from the 7x3.5km pixel. However, some grid cells (2x2km) have multiple pixels overlapping the grid cell, which means that the percentage of the total that it overlaps is the weight that the value has in the 2x2km grid cell. The regrided grid cells are made using weighted values from the pixels. This indicates that if 2 cells (7x3.5km) overlap one grid cell (2x2km) than the percentage that they overlap is taken into account for calculating the weights. Moreover, the grid cells need to have a coverage of the 7x3.5km cells for at least 50%. Otherwise, they are left empty and acquire the fillvalue.

After using the quality flags, for each time period the orbits were aggregated and averaged. The timeseries consists of 10 orbits and 47-70 orbits for the one week (for 23rd – 29th June 2019) and one season (June – August 2019), respectively. All orbits were aggregated and showed a aggregated mean value for the time period of one day (28th June 2019), one week (23rd – 29th June 2019) and one season (June – August 2019).

Additionally, KNMI also calculated the flux and divergence from the Sentinel-5P data. For each time period the flux was calculated per orbit. Afterwards, the divergence was calculated per orbit and then the divergence was aggregated over the time period. A detailed description of the methods for this calculation can be found in *Chapter 3.1*.

5. METHOD

In this chapter, it is briefly summarised what methods have been applied for each Research Question (RQ). Section 5.1 describes the methods used for identifying the locations of major contributors using concentrations from Sentinel-5P, section 5.2 explains the application of the Beirle method onto Sentinel-5P's and ECMWF's data. Finally, Section 5.3 describes how to answer the questions about the minimal time needed for meaningful emission images and how this compares to an independent bottom-up emission estimates such as TNO-CAMS and the Dutch EmssieRegistratie maps for the Netherlands.

5.1 Interpretation of emissions from NO₂ concentrations in the Netherlands

- *RQ 1 - Is it possible to identify the known emission sources using the total NO₂ tropospheric column measurements?*

For the first Research Question (RQ1) we inspect the NO₂ tropospheric column of Sentinel-5P and investigate if the observed NO₂ peaks correspond with the locations of already known sources of NO₂. A list of well-known CO₂ contributors in the Netherlands acquired from EmissieRegistratie was shown in a graph and its corresponding location was labelled in the NO₂ averaged concentration maps for one season (June – August 2019). And a visual inspection of the NO₂ tropospheric column measurements of Sentinel-5P was done between one day (28th June 2019) and one season (June, July & August 2019).

5.2 Application of the method on Sentinel-5P's data and ECMWF's data

- *RQ 2 - Does our independent implementation of the method reproduce the results presented in Beirle et al. (2019)?*

In RQ 2 images of Beirle et al. (2019a) was reproduced using the method described in (Beirle et al., 2019a). This method is applied to the one season (June, July & August 2019) image of concentration for Riyadh. This method was applied using the equations (3.1 & 3.2) from (Beirle et al., 2019a). According to Beirle et al. (2019a) τ is $4 \cdot 3600$ [s], the factor of L is 1.32 and the fraction of NO₂ is $1/L$.

First, the regridded concentrations was multiplied by the wind vector in two directions (x,y) to create a flux map. This was done for each orbit Afterwards a gradient was applied to each orbit in both directions (x,y) that resulted into the divergence [$\text{mol m}^{-2} \text{s}^{-1}$] per orbit. Adjacent pixels in both directions are taken into account to calculate the divergence. Each divergence was then aggregated according to its time period. Meaning that for one week, all the orbits for each pixel are aggregated over one week's time. This is done for one season as well. Sinks were calculated using the vertical column of NO₂ [mol m^{-3}] divided by τ [m s^{-1}]. Afterwards this divergence was

combined with the sinks [mol m⁻² s⁻¹] according to (Beirle et al., 2019a), which resulted in an estimated emission E. (eq. 3.1 and 3.2).

Since (Beirle et al., 2019a, 2019b) uses concentrations and emissions of NO_x instead of NO₂, a conversion between the two must be made. The same units are used in eq 5.1a and 5.1b as in eq. 3.1 and 3.2. Moreover in this paper, a conversion is also made from mol to kg, to compare the images of Beirle et al. (2019a) with this paper's results. The molar weight of NO₂ is 46 g whereas for NO_x it is 30 g. The molar weight for NO_x is :

$$NOx_{molweight} = \frac{1}{L} * NO2_{molweight} + \left(1 - \frac{1}{L}\right) * NO_{molweight} \quad \text{eq. 5.1a}$$

$$E_{\mu g m^{-2} s^{-1}} = (S + D) * NOx_{molweight} \quad \text{eq. 5.1b}$$

The emissions for NO_x were first calculated in [mol m⁻² s⁻¹] and converted using the molar weight of NO_x (eq. 5.1a & 5.1b). This resulted in a map in which emissions have the unit of [μg m⁻² m⁻¹]. A qualitative and quantitative inspection is done for the produced image considering the scale and its values as well as the relation between the values in comparison with image from Beirle et al. (2019a).

- *RQ 3 - What is the optimal height for the wind to be used to determining emissions for the Netherlands and elsewhere?*

Research Question 3 investigated the optimal height for this study's produced images for emissions of the Netherlands. Before the optimal height can be determined, the behaviour of wind in the vertical column and through time was studied. First, using Panoply 4.11.3 the wind's Planetary Boundary Layer (PBL) was visually inspected, particularly how the PBL evolved over time during a day. Using Python 3.7, a plot was made of the wind speed at different altitudes for different times. Third, the wind at 12UTC at different levels was inspected using Panoply 4.11.3. At last, the general pattern of the wind speeds and direction was visualised in a panel with multiple altitudes.

The information mentioned before was used in the final steps for determining the altitude needed for the Beirle method. In the week of 23rd – 29th June 2019, for 26th and the 27th June 2019, the NO₂ plumes above Paris and coastal area of the Netherlands were taken as an example to determine the best fitted altitude for Paris and the Netherlands. From the ECMWF's NetCDF wind files the u and v components for the winds were extracted and transformed into ILWIS datafiles using GDAL. For one day, the file had 31 model levels (107-137), 24 hours (00-23) and therefore 24*31=744 bands per day. So for every 31 bands the same hour but a different model level is

represented. The bands were converted into one map using ILWIS 3.86 according to their model level and hour. Since both u and v are components of a vector, equation 5.2 was used to compute wind speeds:

$$wind_{uv} = \sqrt{u^2 + v^2} \quad \text{eq. 5.2}$$

In ILWIS 3.86, the bands (for 12UTC) of the particular days were combined for the wind vectors for different levels using eq. 5.2. The levels were displayed together with the NO₂ concentration of that particular day for Paris and the Netherlands. For each day, the NO₂ concentrations were compared with the direction and speed of the wind for different levels. The wind direction and speed was used as layer and portrayed over the NO₂ concentration images. The best visual fit was chosen as the best altitude for that corresponding NO₂ plume. Plumes situated over Paris and the west coast of the Netherlands were studied for choosing the optimal altitude. This altitude was used in calculation for the flux and divergence.

5.3 Analysis of emission estimates

- *RQ 4 – What is the minimal integration time that can be used to obtain a useful map for emission estimates?*

A comparison is made between the images for concentration and divergence for Netherlands for one day (28th June 2019), one week (23 – 29 June 2019) and three months (June, July and August 2019). The same approach was used for Riyadh for the same week and the same three months. A visual analysis is done for both groups of images.

- *RQ 5 - How does the method of Beirle compare to independent emission estimates for the Netherlands?*

The image of emissions for Netherlands for 3 months was shown in QGIS 3.12 and overlayed over a satellite imagery that shows urban build-up. Furthermore, a comparison is made with the Dutch EmissiRegistratie inventory (2017) and the Copernicus Atmospheric Monitoring Service (CAM5) - TNO emission inventory for Europe (2016).

6. RESULTS

6.1 Interpretation of emissions from NO₂ concentrations in the Netherlands

- *RQ 1 - Is it possible to identify the known emission sources using the total NO₂ tropospheric column measurements?*

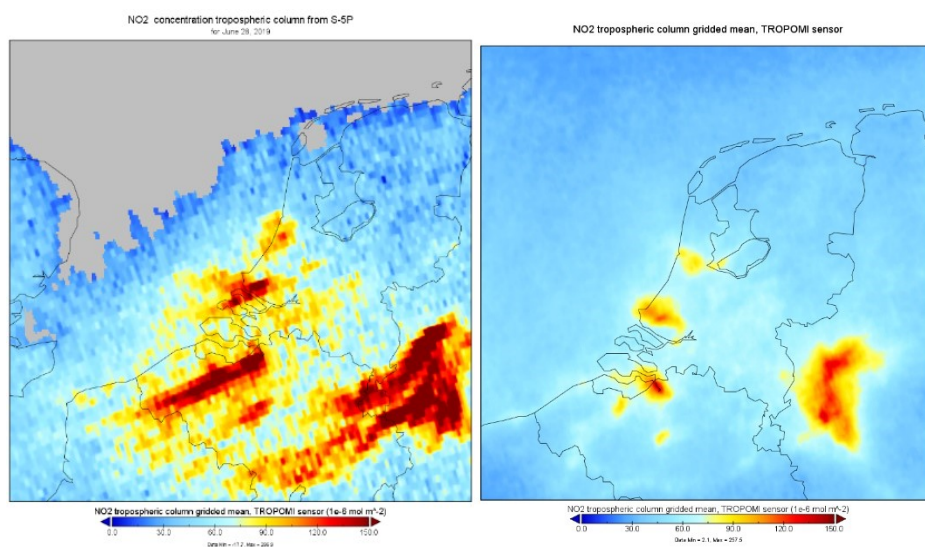


Figure 6-1 - NO₂ concentration measured by TROPOMI. aggregated over their time period, on the left for one day for 28th June 2019 and on the right for one season (June, July and August 2019), both on a 2x2km spatial resolution.

2019, A North-East wind transports the concentrations from the Ruhr area over a distance of 100-200 km to the south-west. When averaging over a greater period of time, the transportation of the NO₂ is average out in all directions it is transported.

As seen in Figure 6-1, a greater time span for averaging results in averaging out the plumes that coincide with daily concentration. High concentrations are most often found above cities and industrial areas.

Larger cities such as London and Paris but also Harbours such as Amsterdam Harbour, Rotterdam Harbour and Antwerp Harbour are within the area of high concentration. For this particular day, 28th June

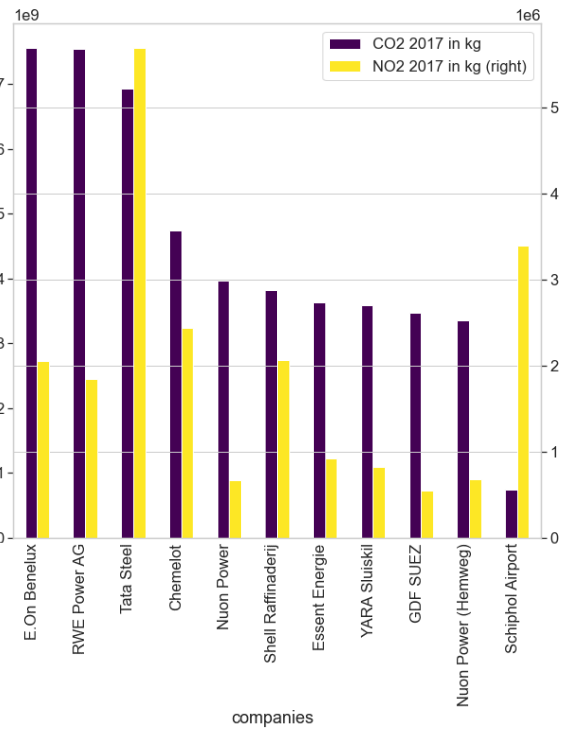
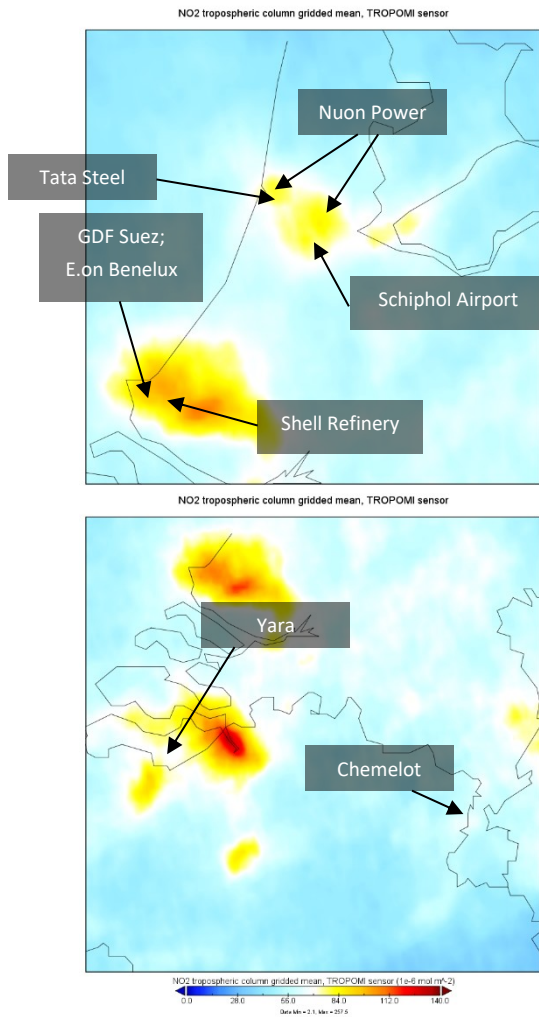


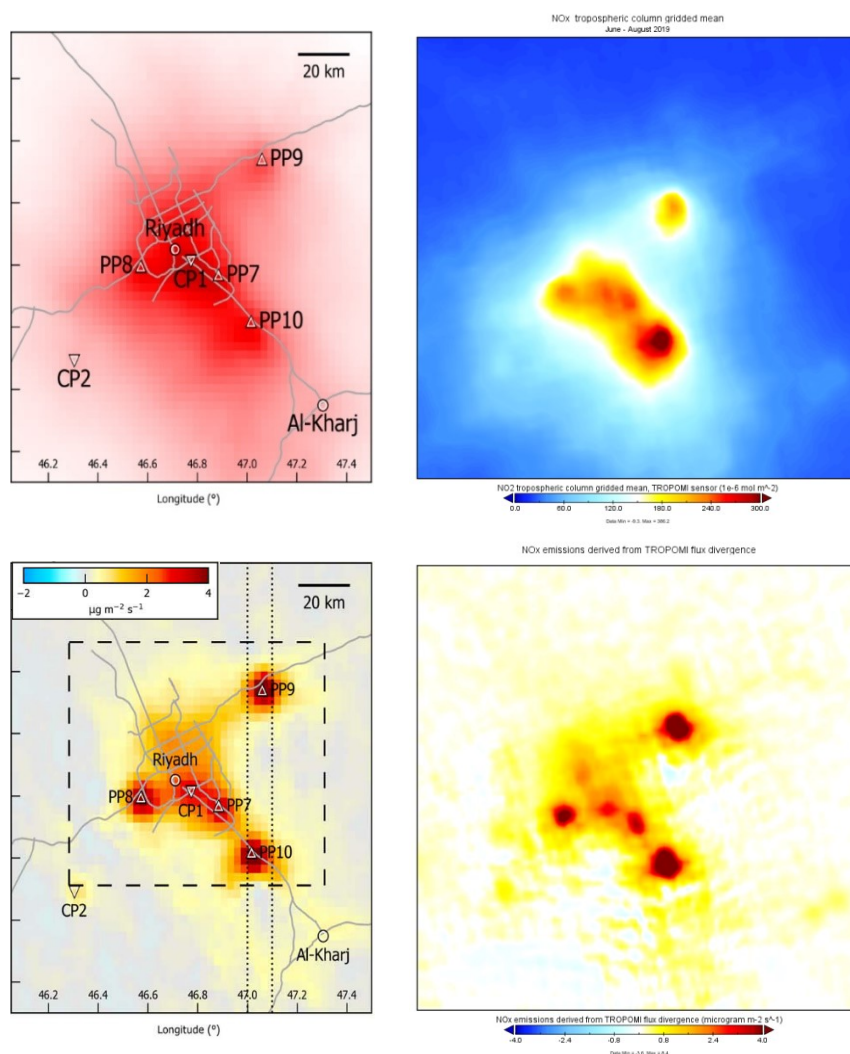
Figure 6-2 - labelled places of high contributors to CO2 and a bar chart with companies and their emissions for 2017 for CO2 and NO2 according to EmissieRegistratie.

In Figure 6-2, the companies that are known for contributing to CO2 in the atmosphere are labelled in their corresponding location. Almost all top-10 contributing companies of CO2 are located in the areas with high NO2 concentrations (>84 *1e-6 [mol m-2]), except for Essent Energie (Geertruidenberg) and Chemelot (Geleen). Those two companies are represented by the colour white in the map (56 – 84 *1e-6 [mol m-2]). Out of the eleven companies listed in the graph, only RWE Power AG (Ems Harbour) is not represented in the NO2 concentration map. The amount of NO2 emitted by RWE Power AG is more than the amount emitted by Yara and GDF Suez combined, however RWE Power AG is not seen in the map whereas Yara and GDF Suez are. Almost all well-known CO2 emitters are shown on the NO2 map regardless of differences in years.

In the next section, the results from the Beirle method is shown together with the altitude of the wind.

6.2 Application of the method on Sentinel-5P's data and ECMWF's data

- RQ 2 - What is the optimal height for the wind to be used to determining emissions for the Netherlands and elsewhere?



In Figure 6-3, the averaged concentration from Beirle is similar to the averaged concentration for the three month period (June, July & August 2019) from this study. The output of emissions from Beirle for Riyadh and this study's emission map are the bottom two images of Figure 6-3. These two images are not only similar in quality but also in quantity. The images have the same spatial distribution of emissions as well as the same range of values in the same unit [$\mu\text{g m}^{-2} \text{s}^{-1}$].

Comparing concentrations with their emission counterpart shows that emissions represent a better distinction spatially between the sources than concentration does.

Figure 6-3 – Images of Beirle et al. (2019) averaged over December 2017 – October 2018 on the left and this study's images averaged over June – August 2019 on the right, where top two images are concentrations derived from Sentinel-5P and bottom images are emissions derived from Sentinel-5P.

- RQ 3 - What is the optimal height for the wind to be used to determining emissions for the Netherlands and elsewhere?

This RQ will be answered by the sections below. First, results will be shown for the change in time. Second, results of change in the vertical column will be shown and lastly, which winds fit best for an example plume.

IMPORTANCE PLANETARY BOUNDARY LAYER

In the next set of images (Figure 6-4) the Planetary Boundary Layer (PBL) is displayed. In essence the PBL is a layer that is close to the surface where the flow is turbulent. The turbulence is created by wind shear and convection of wind. In this layer, vertical mixing of wind is present. Winds do not change rapidly with increasing altitude due to the PBL. Above the PBL, winds are able to change rapidly due to the stratified atmosphere and separated vertical layers. Figure 6-4 shows that the PBL changes with time throughout the day. Therefore the timestamp at which the wind speed are taken into the method of Beirle also plays a significant role.

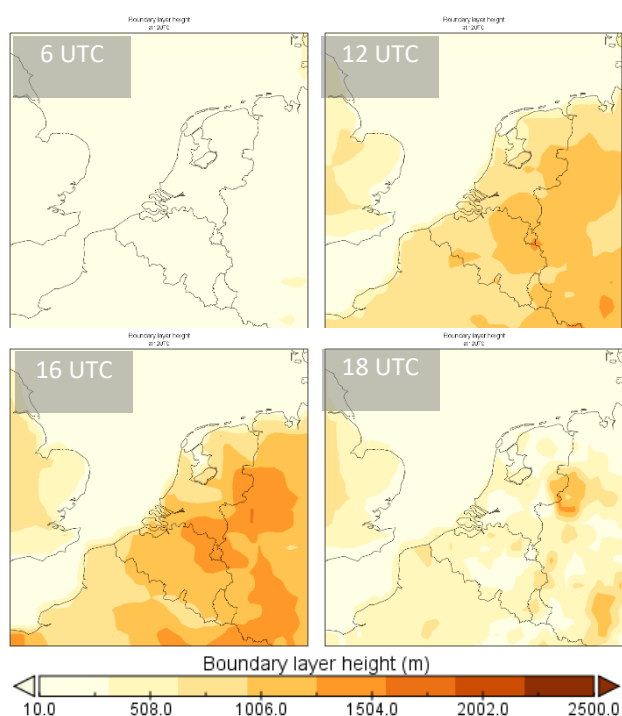


Figure 6-4 - Planetary Boundary Layer for 29th June 2019, for 6, 12, 16 and 18 UTC.

The PBL indirectly acts as a boundary for the altitude of the wind and is influenced by surface roughness and temperature (Mason & Thomson, 2015; Stensrud et al., 2015). In general, the PBL increases during the day and decreases during the night (Figure 6-4). In Figure 6-4, the Planetary Boundary Layer (PBL) is shown for different times (6, 12, 16 & 18 UTC). Over land the PBL changes dramatically as opposed to over sea.

Figure 6-5a shows the altitude of the boundary layer for 29th of June 2019 at 12h00 UTC, acquired from ECMWF. The location is crucial for the Planetary Boundary Layer (PBL), since over sea, the PBL does not rise in altitude throughout the day.

In Figure 6-5b different hours are displayed in a wind speed (x-axis) – altitude (y-axis) graph. This relation for 6, 12 and 16 UTC is displayed in green, black and red respectively. Figure 6-5b only shows the differences between the hours displayed for specific area in East Netherlands-West Germany that has a relative homogeneous Planetary Boundary Layer. The hour for the wind data must be at 12 UTC, since Sentinel-5P has its overpass at roughly between 11h00-13h45 local time. Looking at the Planetary Boundary Layer, the level that is best fitted will not be of greater altitude than 1000m, since for most UTCs the mixing of wind happens at 1000m or lower. For the coastal areas, a different wind altitude is needed as is seen in the boundary layer in Figure 6-5a.

Due to its mixing present in the PBL, average wind speed does not increase with altitude in a smooth line (Figure 6-5b). This means that, above the PBL there is a rapid decrease and underneath the PBL there is a gradual increase in speed (Figure 6-5b), which is indicated with a solid line in its corresponding colour.

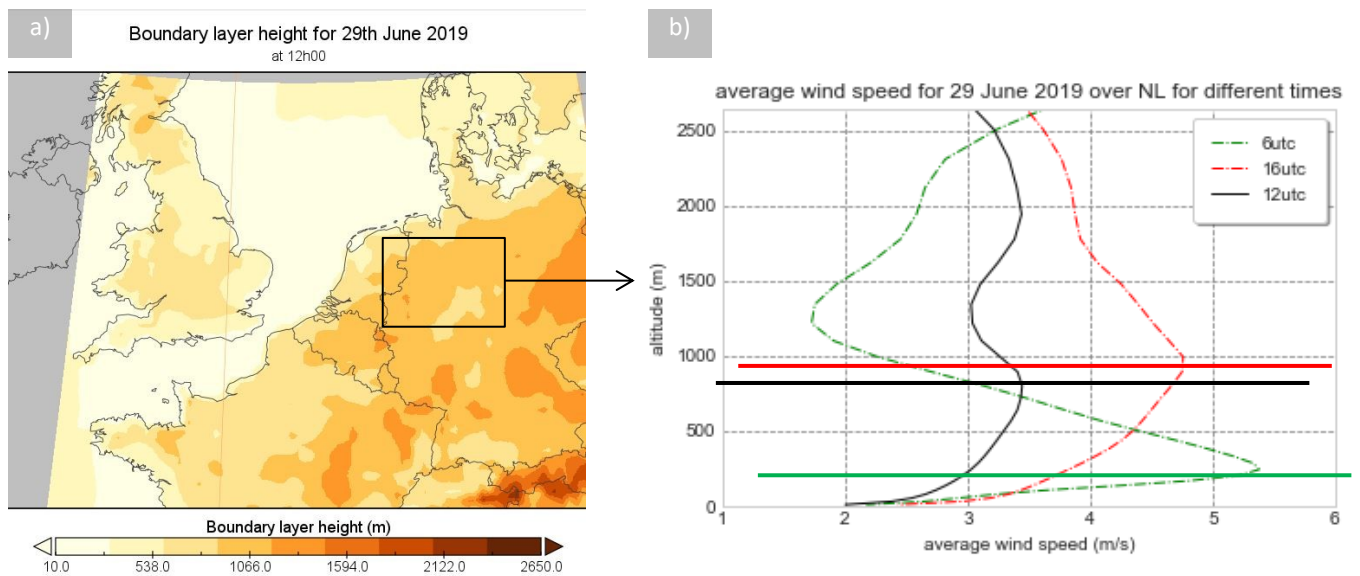


Figure 6-5 - a) Planetary Boundary Layer and b) the average wind speed for different times both for the 29th of June 2019

WIND CHANGES IN THE VERTICAL COLUMN

In Figure 6-6a-e, with increasing altitude the wind speed increases and the direction changes from west to south above the Netherlands. Shades of blue represent the wind speed and the arrows represent the direction (Figure 6-6). The wind changes gradually its direction with increasing altitude and speed. Above sea the change in direction and speed is far stronger than over land in the lowest 1-2 km of the atmosphere.

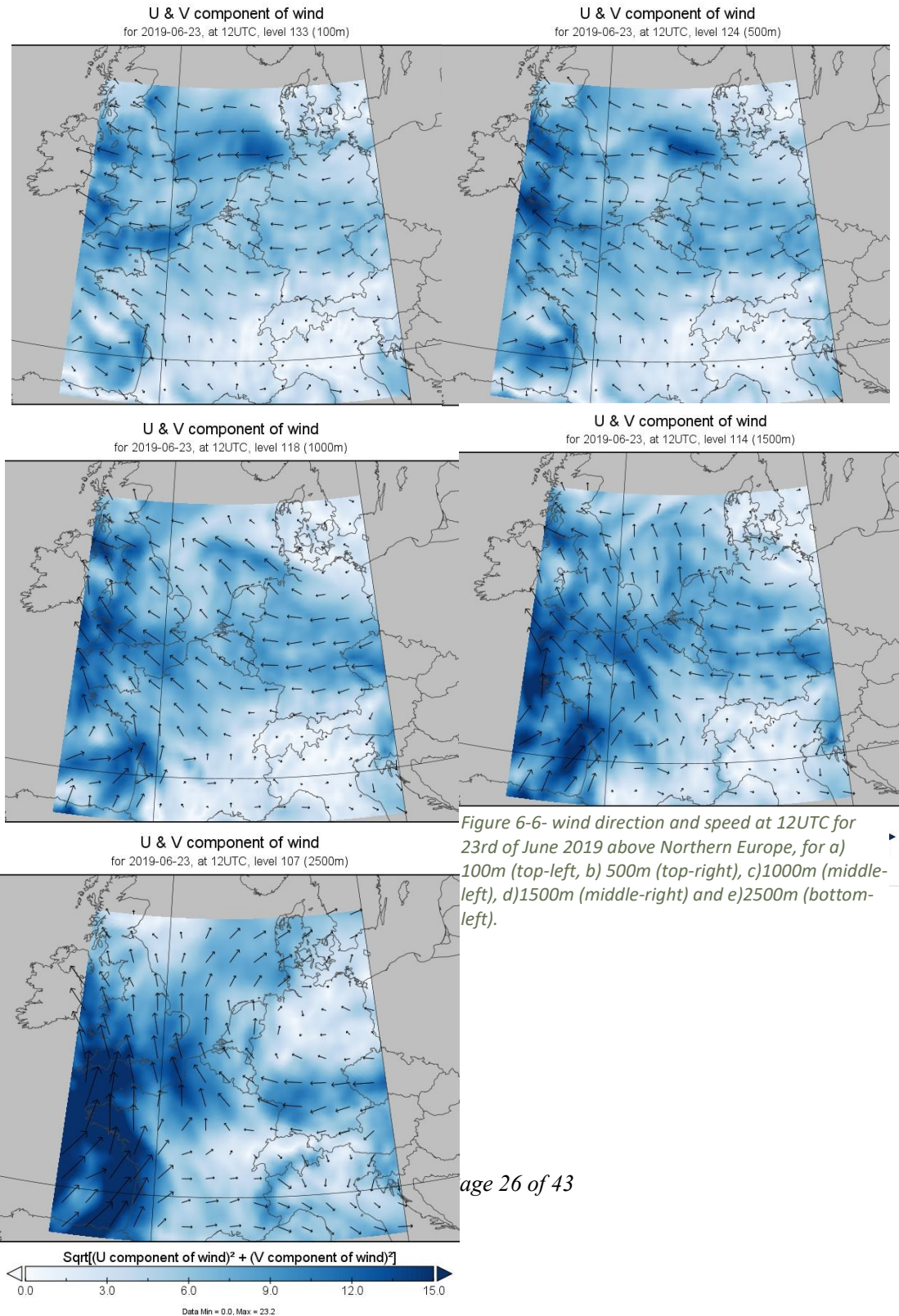


Figure 6-6- wind direction and speed at 12UTC for 23rd of June 2019 above Northern Europe, for a) 100m (top-left), b) 500m (top-right), c)1000m (middle-left), d)1500m (middle-right) and e)2500m (bottom-left).

Figure 6-7a-f shows for 26th of June 2019 the NO₂ concentrations of Sentinel-5P and ECMWF's operational wind data over Paris, France. In Figure 6-7 the same change in direction and speed is shown as in Figure 6-6 for Paris, 26th of June 2019 (Figure 6-7). A general visual representation is done to determine which level best fit the plume's direction.

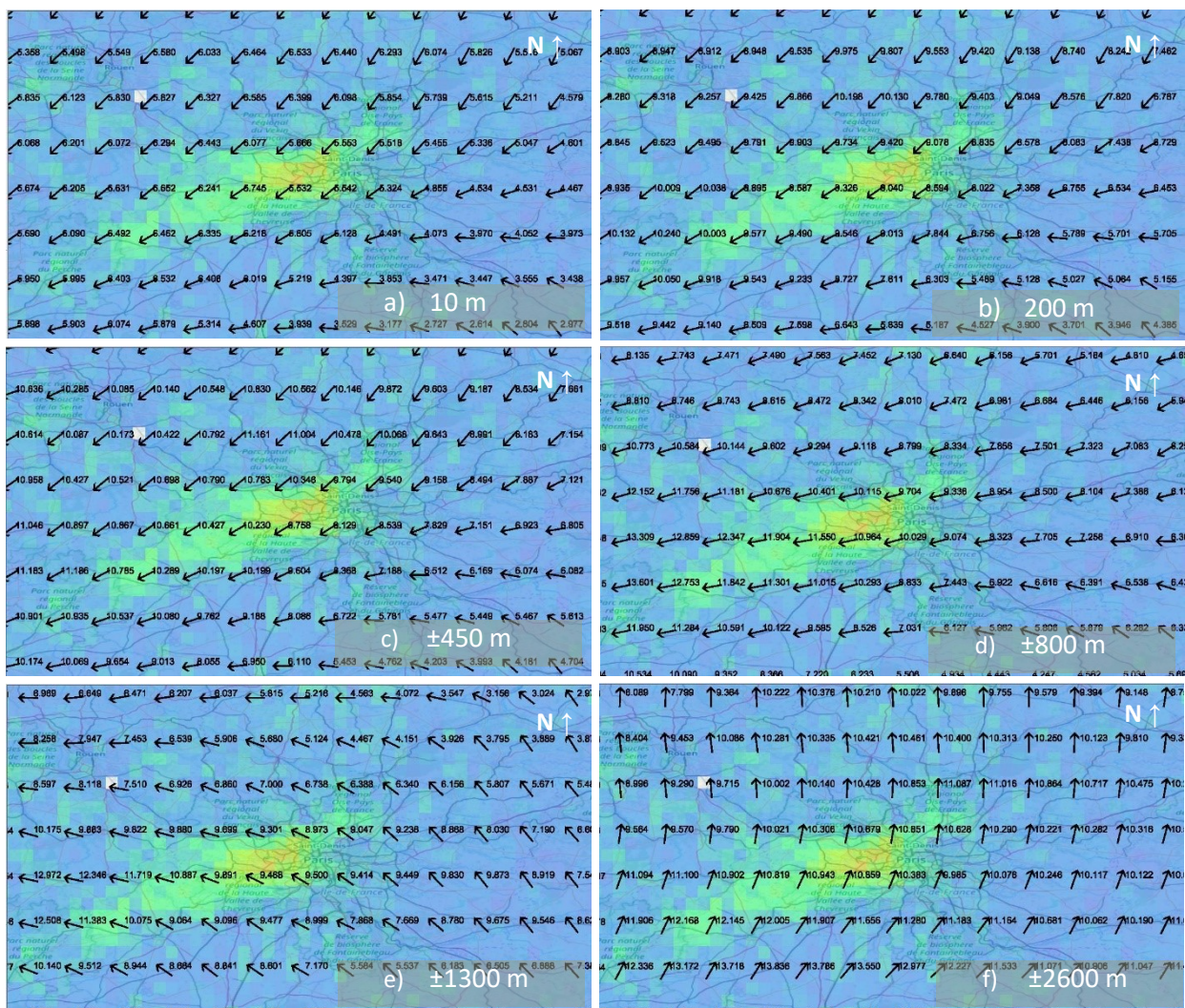


Figure 6-7 - the panels show different wind directions and wind speeds according to different altitudes in meters. This figure shows winds on altitudes from 10 – ±2600 m for 26th of June at 12h00 over Paris. Arrows give wind direction and the number gives wind speed in km/h. The corresponding levels are from ECMWF's model levels. a) 10m (level 137), b) 200m (level 130), c) 440m (level 125), d) 798m (level 120), e) 1328m (level 115) and f) 2653m (level 107).

In general, the direction of the winds are according to the NO₂ plume from 10m – ±450m (level 137-120; Figure 6-7a-d). Accordingly, the direction of the wind changes after ±450m and with it the wind speed decreases until the direction changes again at ±2600m (Figure 6-7e-f). At the surface (10m, Figure 6-7a), the wind transports NO₂ in the right direction however the wind speed is not enough to transport the NO₂ over such a long distance. Within the Planetary Boundary Layer (PBL), 200-800m, the wind vectors are in the same direction as the NO₂ concentration (Figure 6-5 & Figure 6-7) From ±800m onwards, above the PBL, the wind speed decreases and the direction deviates from the overall direction of the NO₂ concentrations. The optimal wind altitude, therefore, must be within the PBL.

Figure 6-8a-d shows the altitudes between 500m – ±700. In these images (Figure 6-8), two arrows are drawn; the direction of plume (white) and the direction of the wind (yellow). The images in Figure 6-7c and Figure 6-7d are similar. This reveals that differences between the altitudes of 500m – ±700m are small (Figure 6-8a-d). For the

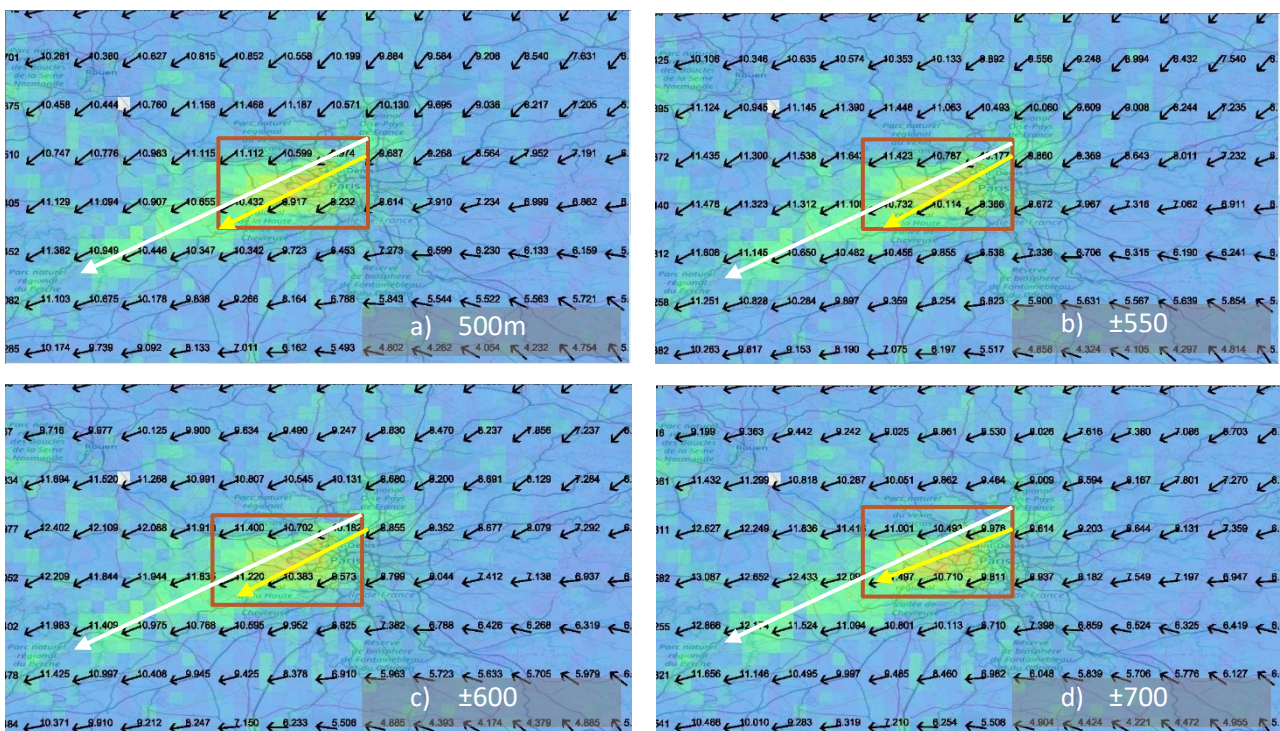


Figure 6-8 - the panels show different wind directions and wind speeds according to different altitudes in meters. This figure shows winds on altitudes from 500 – ±700m for 26th of June at 12h over Paris. White arrow give direction of the plume, and yellow arrow give direction of overall wind direction, the number gives wind speed in km/h. The corresponding levels are from ECMWF's model levels. a) 500m (level 124), b) ±550m (level 123), c) ±600m (level 122) and d) ±700m (level 121). These panels can be placed between fig. 6-8c and 6-8d.

Beirle method, it would be sensible to use $\pm 450\text{m}$ for the wind altitude because the winds have lower values than 500m and are progressing in the same direction as NO₂ concentrations.

As is described above, the altitude of 450m would best work for Paris and according to Beirle et al. (2019a) for Riyadh and Germany as well. The circumstances near the Dutch coast is complicated. As was shown in Figure 6-4, the Planetary Boundary Layer along the coast does not change as dramatically as above land. This is due to lower temperatures above sea compared to temperatures above land. This causes a thinner PBL and it has less turbulence within (Malda, De Arellano, Van Den Berg, & Zuurendonk, 2007). In the next set of images (Figure 6-9), multiple wind altitudes are shown for the coast of the Netherlands.

In Figure 6-9, winds are shown with altitudes from 10 – 200m. The wind at 10m (Figure 6-9a) goes from South-East and bends towards West and changes at $\pm 100\text{m}$ (Figure 6-9c) to a North-West-wind. Above sea, the wind direction changes dramatically with increasing altitude, at such a rate that the optimal altitude for coastal areas is

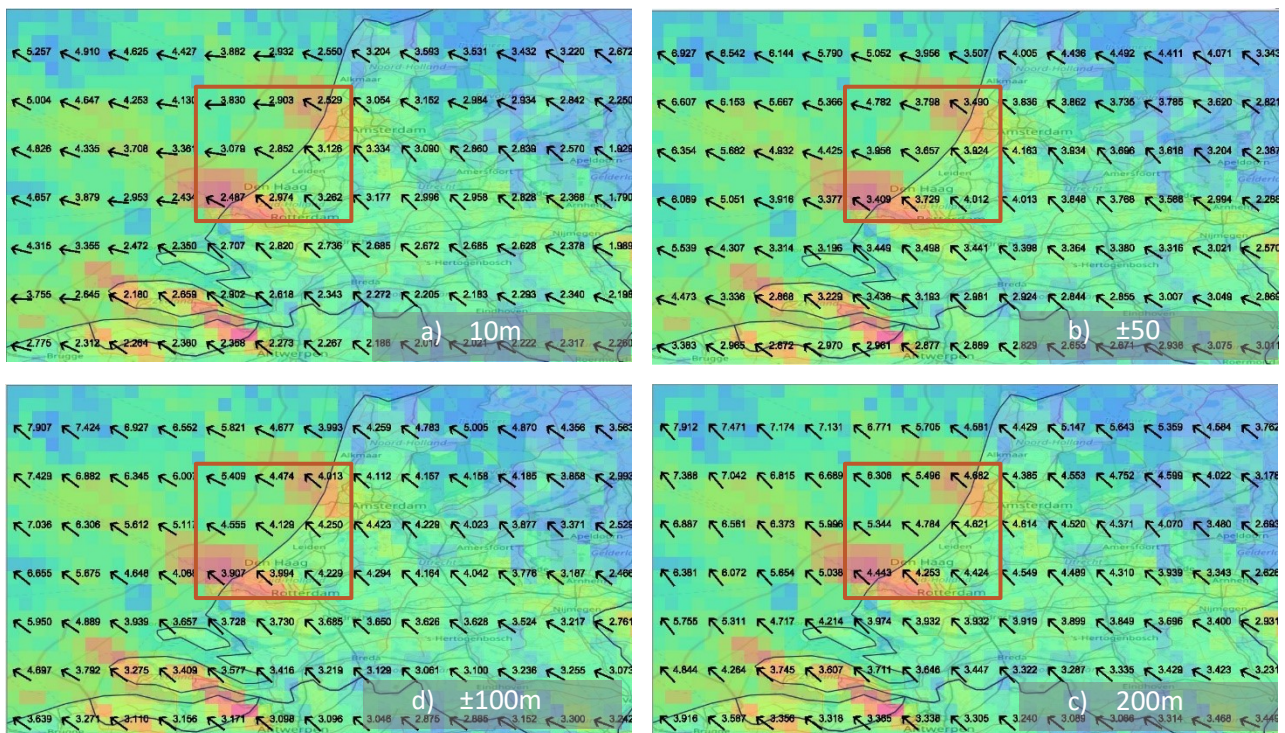
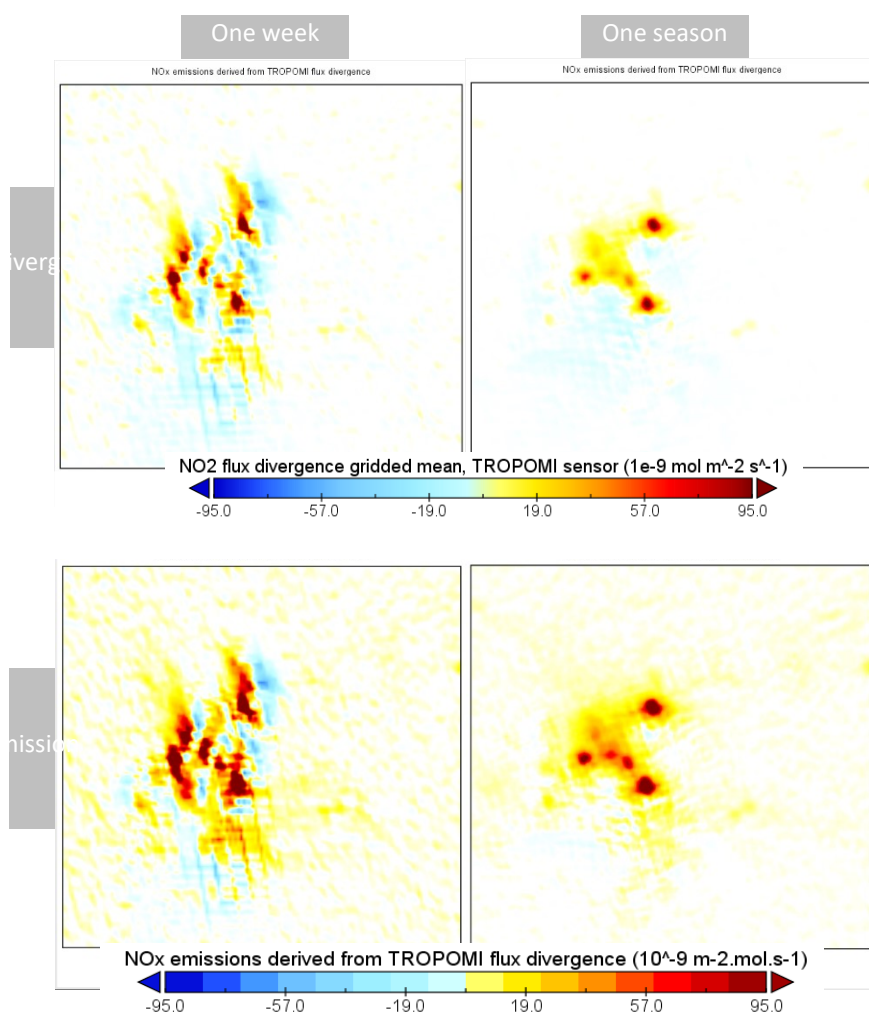


Figure 6-9 - the panels show different wind directions and wind speeds according to different altitudes in meters. This figure shows winds of altitudes from 10 – 200m for 27th of June at 12h over the coast of the Netherlands with NO₂ concentrations underneath the arrows. Arrows give wind direction and the number gives wind speed in km/h. The corresponding levels are from ECMWF's model levels. **a)** 10m (level 137), **b)** $\pm 50\text{m}$ (level 135), **c)** $\pm 100\text{m}$ (level 133) and **d)** 200m (level 130).

between 50-200m. As mentioned previously, the range for the optimal altitude over land is greater (450-800m) than for sea. Hence, for the entire Netherlands, a general wind altitude of 450m would be preferable.

6.3 Analysis of emission estimates

- *RQ 4* – What is the minimal integration time that can be used to obtain a useful map for emission estimates?



For this section, the results from the Beirle method is shown for Riyadh and for the Netherlands and Northern Europe for one day (28th June 2019), one week (23rd – 29th June 2019) and one season (June, July and August 2019).

For Riyadh in Figure 6-10 the fluxdivergence and emissions for a week and three months are shown. In this figure, a clear distinction for fluxdivergence and emissions can be seen between one week and one season. For the three month period, the fluxdivergence and the emissions shows well-defined point sources. The weekly average shows these point sources clearly although, they also illustrate the features related to the plume structure.

Figure 6-10 - fluxdivergence & emission for one week (23 - 29 June 2019) and one season (June, July & August 2019).

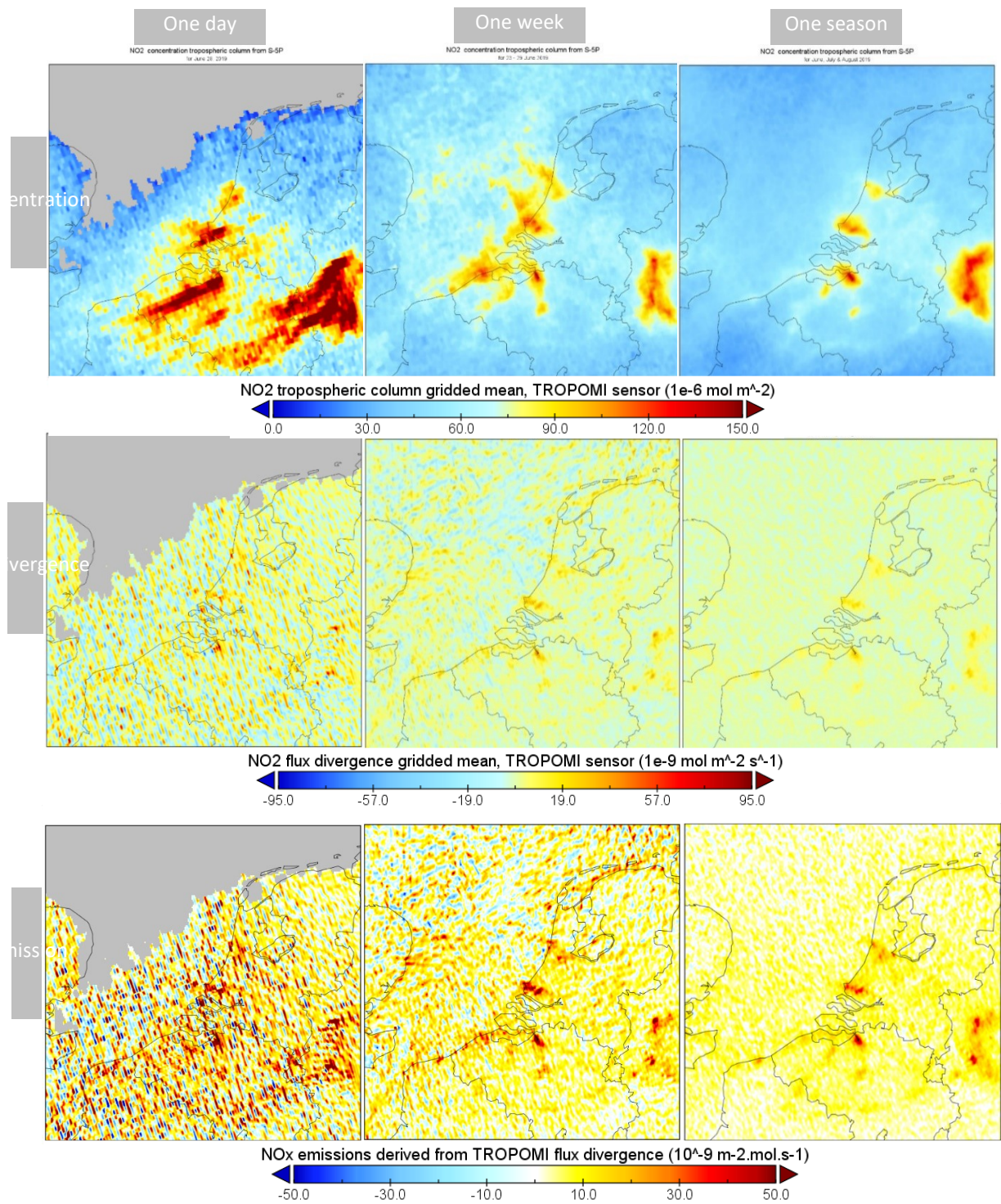


Figure 6-11 – concentrations, fluxdivergences and emissions for one day (28 June 2019), one week (23 – 29 June 2019) and one season (June, July & August 2019).

A 3x3 grid (Figure 6-11) is shown with the temporal averaging in columns and the phase in the method (concentration, fluxdivergence and emissions) in rows. In general, the noise decreases with increasing time-averaging for concentration, fluxdivergence and emissions. Concentrations narrow the possible location of the sources with increasing temporal averaging.

For the weekly averaged maps, the fluxdivergence and the emissions are more visible compared to the daily average maps, however there is still a fair amount of noise present in images. For emissions, the three month period has the least amount of noise and shows sources consistent with what to expect from the concentrations for that same period (Figure 6-11). In Figure 6-11, it is shown that for the Netherlands the minimal amount of time for averaging and integrating that is needed to create an image with emission sources is at least three months.

- RQ 5 - How does the method of Beirle compare to independent emission estimates for the Netherlands?

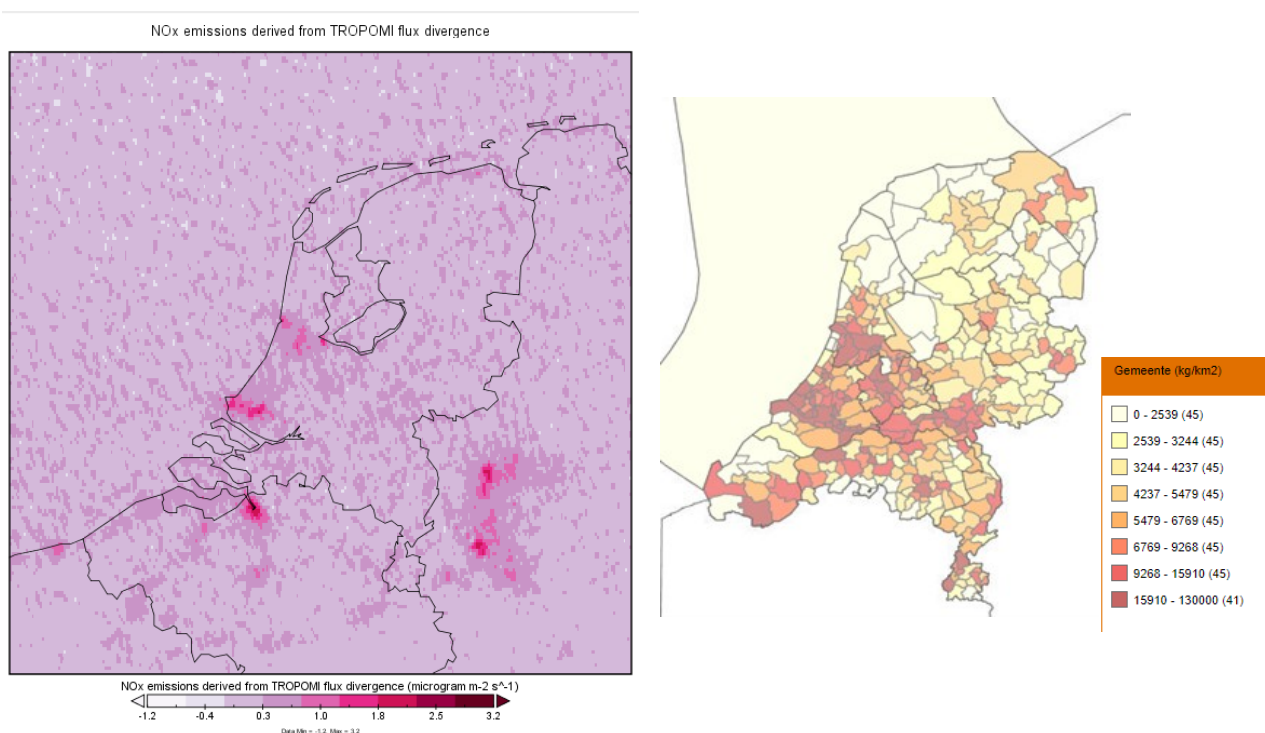


Figure 6-12 - emissions from one season (June, July & August 2019) on a 2x2km grid (left) and emission per municipality from EmisRegistatie (2017) (right).

Figure 6-12 shows both emissions derived from Sentinel-5P [$\mu\text{g m}^{-2} \text{s}^{-1}$] and emissions from EmisRegistatie.nl [kg km^{-2}]. The type of representation is different: EmisRegistatie shows per

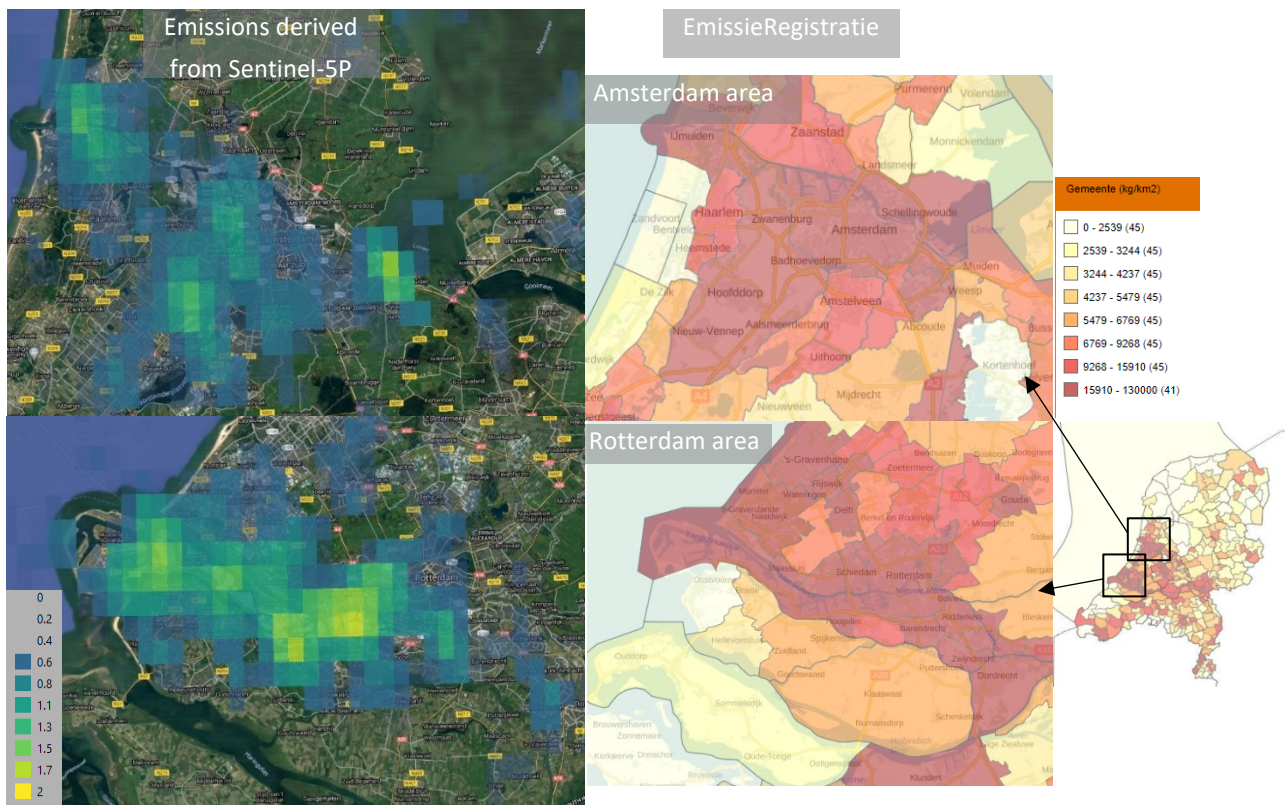


Figure 6-13 - images of emissions derived from Sentinel-5P (left) [$\mu\text{g m}^{-2} \text{s}^{-1}$] and images from EmissieRegistratie (right) [kg km^{-2}] with focus on Amsterdam area (top) and Rotterdam area (bottom).

municipality and not per gridcell ($2 \times 2 \text{ km}$). Furthermore EmissieRegistratie shows for one year whereas this study's map shows one season in units [$\mu\text{g m}^{-2} \text{s}^{-1}$]. And lastly, the colours used in EmissieRegistratie does not show the absolute emission estimates but in comparison to the other municipalities.

As a result, the image of EmissieRegistratie and this study's one season image is not comparable. However, it is possible to compare the municipalities with the brightest colour (dark red) with the highest values in this study image. The location of the sources to concur in both images. The Amsterdam area and the Rotterdam area are represented in both images (Figure 6-12).

In Figure 6-13 zooms in on the Amsterdam area and the Rotterdam area with the Sentinel-5P's emission estimates from one season. In general, the emissions derived fit the overall pattern of EmissieRegistratie. Since EmissieRegistratie shows a larger area due to using municipalities instead of point sources, a municipality can be influenced by one or more point sources.

In Figure 6-14, the Sentinel-5P emission estimates for one season (June – August 2019) are shown next to the total emission estimates from CAMS for 2016. The Sentinel-5P emission estimates and the CAMS estimates have the same absolute values [$1 \cdot 10^{-12}$ kg m⁻² s⁻¹]. In Figure 6-14, on the left Sentinel-5P emission estimates and on the right CAMS emission inventories are shown with different scales to emphasise the noise and show the overall patterns.

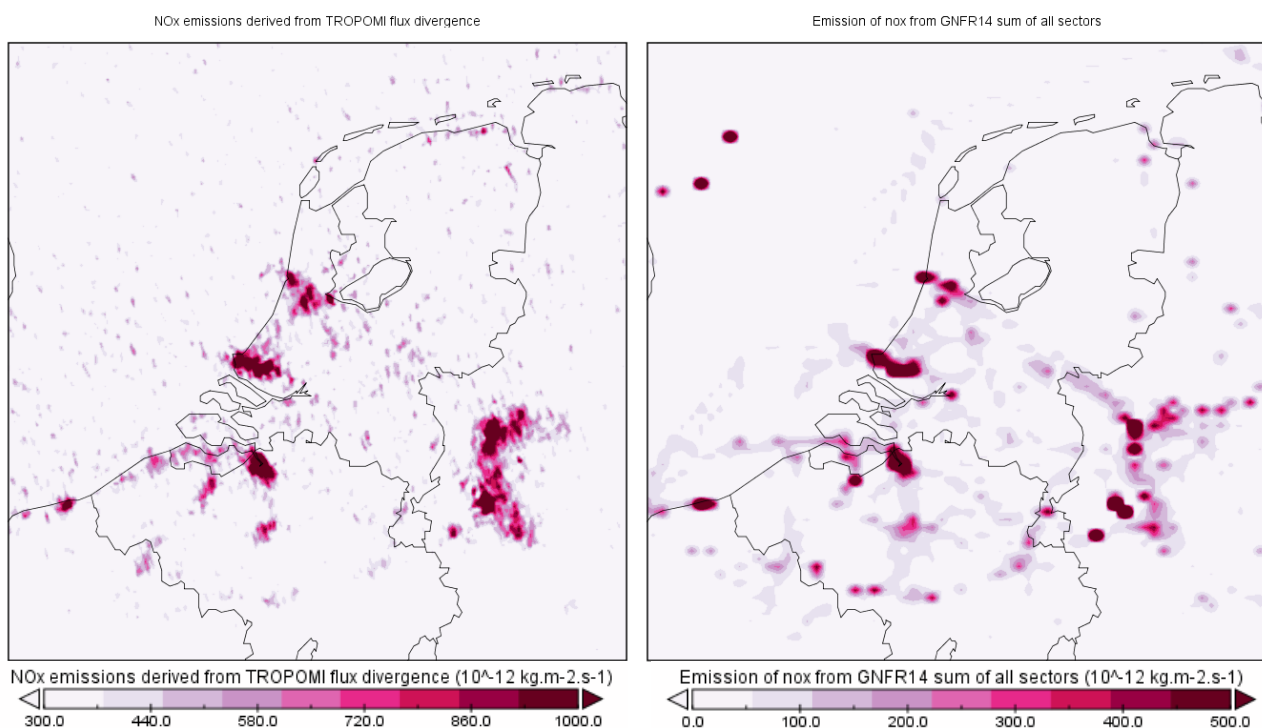


Figure 6-14 - comparison between Sentinel-5P and CAMS emission estimates at different scales.

In general the overall patterns with the highest values in both estimates are comparable. However, the values for Sentinel and CAMS are different. For CAMS waterborne transport is slightly visible within a range of 0 – 500 [10^{-12} kg m⁻² s⁻¹], whereas for Sentinel-5P, there is too much noise to see a distinctive pattern. The high values of

CAMS correspond with the high values of Sentinel-5P when neglecting the noise and medium level values in between the high value locations (Figure 6-14). Amsterdam area, Rotterdam area, Antwerp and industrial Ruhr area are present in both emission estimates. The patterns seen in Sentinel-5P concur qualitatively and quantitatively with CAMS, regardless of noise.

7. DISCUSSION

In general the method of Beirle et al. (2019a; 2019b) highly depends on the altitude for the wind data. And it depends on the resolution of the wind data and the Sentinel-5P data. Sentinel-5P has a resolution of 7x3.5km, using regriding. By averaging over time and oversampling on a 2x2km grid, the Beirle method creates features that are scaled down, than using Sentinel-5P's data directly. The Beirle method has been implemented on the oversampling grid of 2x2 km and enables it to be used on smaller areas such as the Netherlands, Riyadh and cities and their neighbouring towns such as Amsterdam and Rotterdam.

- *RQ 1 - Is it possible to identify the known emission sources using the total NO₂ tropospheric column measurements?*

As mentioned in Chapter 6, the concentrations measured from Sentinel-5P does give an indication of emission sources, however this is still spread over a large area. Depending on the wind direction and speed, the concentration from a certain source can travel great distances (order of 100km) as can be seen in Figure 6-1. Concentration is not the same as emission and even with a resolution of 2x2km and a time averaging of one season, this does not give the exact emission within that 2x2km grid. Using the list of CO₂ contributors, it is clear that these contributors are coincidently within the NO₂ concentrations on the map (Figure 6-2). The relation between CO₂ and NO₂ is clearly visible in this figure. Deriving emission can narrow the location of the contributors to a certain extent.

- *RQ 2 - What is the optimal height for the wind to be used to determining emissions for the Netherlands and elsewhere?*

Figure 6-3 shows that the Beirle method is reproduceable, including the conversion of NO₂ to NO_x and the units [mol m⁻² s⁻¹] to [µg m⁻² s⁻¹]. These images do not only compare visually (qualitatively) but also in absolute values (quantitatively). Furthermore these emission images show sharper features than its concentration counterpart. This shows that the Beirle method is capable to isolate individual point sources.

Saudi Arabia has its industry and urban build-up far more dispersed than Northern Europe. The altitude of 450m for Riyadh works, however that does not mean it will work for other study areas as well. Therefore it is indispensable that the altitude for the wind data is checked for the area of interest. In this study, in accordance with Beirle et al. (2019a) a fixed altitude for the wind is used, but this is too high for coastal areas.

- *RQ 3 - What is the optimal height for the wind to be used to determining emissions for the Netherlands and elsewhere?*

Over land, the altitude of $\pm 450\text{m}$ works well for the PBL for summer months, this altitude is roughly within the PBL. Since the PBL is dependent on sea surface temperatures this altitude could change for winter months. Given that the Planetary Boundary Layer (PBL) changes over time throughout the day for land but stays low and stagnant over sea, gives the impression that for coastal areas a different optimal altitude exists than 450m . A better fit for the wind altitude would be between 10 and 200m (Figure 6-9). In this study an overall altitude of 450m was used for the entire Netherlands, which means that it is possible that there is a margin of error for the coastal areas.

In addition to this error, another problem rises as well: the spatial variability of the PBL in the coastal areas due to 1) the temperature due the time of the year (surface temperature), 2) the boundaries of the coastal area. Thus, the scale of the study area is important as well. When using different altitudes for areas within the Netherlands, the border between altitude for the coast and altitude for the rest of the country must be determined, which may vary daily or with each season. Scale, period and location are the important factors to take into account for choosing the right altitude for wind data.

Wind over sea and over land behaves differently, that is mainly due to temperature of sea and land and due to surface temperatures of the sea and of the land. Even though drastic changes can be seen along the coastline, due to the scope of this study an altitude of $\pm 450\text{m}$ was used for the entire Netherlands rather than different altitudes for areas within the Netherlands. Especially over the North Sea, the current implementation shows a lot of noise.

- *RQ 4 – What is the minimal integration time that can be used to obtain a useful map for emission estimates?*

The minimal time that is needed to integrate a statistically sound image varies with location. For Riyadh , one week would be possible, however due to the limited amount of orbits and data, the features seen in plumes from daily NO₂ concentrations still have an effect in the emission estimates map. One season, would be preferable for Riyadh (Figure 6-10).

For the Netherlands at least three months must be used to obtain emission estimates. In the vicinity of the emission sources, there was more noise present in the Netherlands than near Riyadh (Figure 6-10 & Figure 6-11). Certain factors such as high albedo, low built-up density and less cloud cover makes it possible for Riyadh to almost need one week for determining emissions. The Netherlands, on the other hand, has high built-up density, sources close to each other and high cloud coverage throughout the year. Due to cloud coverage alone, averaging over large time periods is necessary. Even though the time period of 23rd – 29th

June 2019 had a particular clear sky, the image of one week was noisy. Location and its factors determine the duration of the time averaged period for deriving emissions.

- *RQ 5 - How does the method of Beirle compare to independent emission estimates for the Netherlands?*

First of all, EmissieRegistratie shows only yearly values of which 2017 is the most recent data, whereas the Beirle method can be applied on numerous time averaging periods if the location permits this. Moreover, the data from EmissieRegistratie is per municipality available even though EmissieRegistratie has 1km x 1km grid data. In this study, the Beirle method is used for one season (June, July and August 2019) whereas EmissieRegistratie is for an entire year. Using the Beirle method, there are more possibilities time-wise.

Second, EmissieRegistratie has more information on the emission sources and their groups. This entails that EmissieRegistratie can give per municipality information about how much mass per area comes from which type of source and to which category it belongs.

Third, the images of emissions derived from Sentinel-5P and EmissieRegistratie (Figure 6-13) are similar in their location of the sources. The EmissieRegistratie maps for municipalities ignore the spatial variability of emission estimates. Within a municipality, the spatial variability can vary as well. For example, for the Amsterdam municipality (Figure 6-13), it matters for the concentration where exactly the emissions are. For a quantitative comparison, the Sentinel-5P image needs to range for an entire year, the same units and using grid cells (1x1km).

Fourth, EmissieRegistratie only has estimated data for the Netherlands, while Sentinel-5P and the Beirle method can be applied to all areas of the Earth on all scales. And Sentinel-5P measures NO₂ rather than EmissieRegistratie estimating the emissions. For absolute values per category of industry and firm, EmissieRegistratie could work, however for time series, closer analysis of emissions of NO_x, for most parts of the Earth, the method of Beirle gives feasible results for further analysis.

Lastly, in Figure 6-14, a qualitative and quantitative comparison was made between the Sentinel-5P emissions estimates (June – August 2019) and CAMS emission estimates (2016). The amount of noise in the Sentinel-5P's emission estimates are due to the τ being $4 \cdot 3600$ [s]. For emissions, the same value of τ is used (eq. 3.1) as in Beirle et al. (2019a), a lower τ would give less noise.

8. CONCLUSION & FUTURE RECOMMENDATIONS

This study aimed to identify emissions for the Netherlands from Sentinel-5P's data and ECMWF's operational data. The Beirle method was independently reproduced and compared to the results from Beirle et al. (2019a). This study illustrates that for different time averaging periods this method can determine emissions, but it also raises questions about which factors complicate the determination of emissions and that this method will work.

In order to use this method, a close look must be provided to the direction of the plumes of NO₂ and the direction of the wind. That is to determine the optimal altitude of the wind to be used for that particular area of interest. It can be concluded that the method described in Beirle et al. (2019a) is able to determine emission sources spatially and quantitatively for different time periods depending on their location.

8.1 Future recommendations

First, the variables used in the Beirle method should be examined in detail. The Beirle method creates noise for Sentinel-5P's 2x2km grid data, due to a greater lifetime (τ) value. For future studies, it would be advised to reduce the τ and see how small τ should be. Emission estimates derived from Sentinel-5P uses a ratio for NO_x/NO₂ defined by Beirle et al. (2019a). A different ratio has an impact on the Sinks and Emissions described by Beirle et al. (2019a) and eq. 3.1 and 3.2. The difference between emission estimates of NO₂ and NO_x can be great or small, depending on the ratio defined.

Second, this study's Sentinel-5P emission estimates have a lot of noise over the North Sea. As has been mentioned, the Planetary Boundary Layer (PBL) is low and stagnant in coastal areas. As the Netherlands has most of its emission sources of NO_x near the coast and wind behaves differently near the coast, it would be interesting to see if a more optimal wind altitude could be determined for the coastal areas. For future studies, this gap might be interesting to explore since it can improve the values acquired from this method. This may also hold for mountainous areas such as the Alpes and the Pyrenees. Beirle et al. (2019a) and this study used summer season data, and in summer the decay time of NO_x is different from the winter. Therefore determining emissions using this method for winter might give other results. The PBL, mountainous areas and season have an effect on emission estimates.

Third, the wind altitude is still up for debate. The altitude depends on many variables: the PBL, temperature and season. And indirectly, this depends on location. That means for the Netherlands, another time period a different altitude would be preferable rather than ± 450 m. For example, for one year the clouded days would not have an

effect on the method. Choosing the optimal altitude would need a different approach taken into account the winter and the summer months.

Lastly, EmissieRegistratie only shows data based per municipality, due to the fact that this was available for this study. A detailed comparison between emission derived from Sentinel-5P and EmissieRegistratie 1x1km grid data's estimations would be preferred for future studies.

9. REFERENCES

- Ahmed Bhuiyan, M., Rashid Khan, H. U., Zaman, K., & Hishan, S. S. (2018). Measuring the impact of global tropospheric ozone, carbon dioxide and sulfur dioxide concentrations on biodiversity loss. *Environmental Research*, 160(October 2017), 398–411. <https://doi.org/10.1016/j.envres.2017.10.013>
- Beirle, S., Borger, C., Dörner, S., Li, A., Hu, Z., Liu, F., ... Wagner, T. (2019a). Pinpointing nitrogen oxide emissions from space. *Science Advances*, 5(11), eaax9800. <https://doi.org/10.1126/sciadv.aax9800>
- Beirle, S., Borger, C., Dörner, S., Li, A., Hu, Z., Liu, F., ... Wagner, T. (2019b). supplement: Pinpointing nitrogen oxide emissions from space. *Science Advances*, 5(11), eaax9800. <https://doi.org/10.1126/sciadv.aax9800>
- Berner, E. K., & Berner, R. A. (2012). *Global Environment: water, air, and geochemical cycles* (second). Oxfordshire: Princeton University Press.
- Boersma, K. F., Eskes, H. J., Richter, A., De Smedt, I., Lorente, A., Beirle, S., ... Compennolle, S. C. (2018). Improving algorithms and uncertainty estimates for satellite NO₂ retrievals: Results from the quality assurance for the essential climate variables (QA4ECV) project. *Atmospheric Measurement Techniques*, 11(12), 6651–6678. <https://doi.org/10.5194/amt-11-6651-2018>
- Dentener, F., Stevenson, D., Ellingsen, K., Van Noije, T., Schultz, M., Amann, M., ... Zeng, G. (2006). The global atmospheric environment for the next generation. *Environmental Science and Technology*, 40(11), 3586–3594. <https://doi.org/10.1021/es0523845>
- Ding, J., van der A, R. J., Mijling, B., Jalkanen, J. P., Johansson, L., & Levelt, P. F. (2018). Maritime NO_x Emissions Over Chinese Seas Derived From Satellite Observations. *Geophysical Research Letters*, 45(4), 2031–2037. <https://doi.org/10.1002/2017GL076788>
- Ding, J., Van Der A, R. J., Mijling, B., Levelt, P. F., & Hao, N. (2015). NO_x emission estimates during the 2014 Youth Olympic Games in Nanjing. *Atmospheric Chemistry and Physics*, 15(16), 9399–9412. <https://doi.org/10.5194/acp-15-9399-2015>
- Eskes, H., Van Geffen, J., Boersma, F., Eichmann, K.-U., Apituley, A., Pedernana, M., ... Loyola, D. (2019). Sentinel-5 precursor/TROPOMI Level 2 Product User Manual Nitrogen dioxide.
- Forster, P. (2007). Changes in atmospheric constituents and in radiative forcing,. *In Climate Change 2007, The Physical Science Basis. Contribution of Working Group I to the Fourth Assessment Report of the Intergovernmental Panel on Climate Change*, 129–234.
- Goldberg, D. L., Lu, Z., Streets, D. G., De Foy, B., Griffin, D., Mclinden, C. A., ... Eskes, H. (2019). Enhanced Capabilities of TROPOMI NO₂: Estimating NO_x from North American Cities and Power Plants. *Environmental Science and Technology*, 53(21), 12594–12601. <https://doi.org/10.1021/acs.est.9b04488>
- Jury, M. R. (2017). Statistics and meteorology of air pollution episodes over the South African highveld based on satellite-model datasets. *Journal of Applied Meteorology and Climatology*, 56(6), 1583–1594. <https://doi.org/10.1175/JAMC-D-16-0354.1>
- Klein, H., Gauss, M., Nyiri, A., & Benedictow, A. (2018). *Transboundary air pollution by main pollutants (S , N ,*

O₃) and PM in 2010.

- Lorente, A., Boersma, K. F., Eskes, H. J., Veefkind, J. P., van Geffen, J. H. G. M., de Zeeuw, M. B., ... Krol, M. C. (2019). Quantification of nitrogen oxides emissions from build-up of pollution over Paris with TROPOMI. *Scientific Reports*, *9*(1), 20033. <https://doi.org/10.1038/s41598-019-56428-5>
- Malda, D., De Arellano, J. V. G., Van Den Berg, W. D., & Zuurendonk, I. W. (2007). The role of atmospheric boundary layer-surface interactions on the development of coastal fronts. *Annales Geophysicae*, *25*(2), 341–360. <https://doi.org/10.5194/angeo-25-341-2007>
- Manders, A. M. M., Builtjes, P. J. H., Curier, L., Gon, H. A. C. D. Vander, Hendriks, C., Jonkers, S., ... Schaap, M. (2017). Curriculum vitae of the LOTOS-EUROS (v2.0) chemistry transport model. *Geoscientific Model Development*, *10*(11), 4145–4173. <https://doi.org/10.5194/gmd-10-4145-2017>
- Mason, P. J., & Thomson, D. J. (2015). Boundary Layer (Atmospheric) and Air Pollution: Overview. *Encyclopedia of Atmospheric Sciences: Second Edition*, *1*, 220–226. <https://doi.org/10.1016/B978-0-12-382225-3.00081-5>
- Mijling, B., & Van Der A, R. J. (2012). Using daily satellite observations to estimate emissions of short-lived air pollutants on a mesoscopic scale. *Journal of Geophysical Research Atmospheres*, *117*(17), 1–20. <https://doi.org/10.1029/2012JD017817>
- Mijling, B., Van Der A, R. J., & Zhang, Q. (2013). Regional nitrogen oxides emission trends in East Asia observed from space. *Atmospheric Chemistry and Physics*, *13*(23), 12003–12012. <https://doi.org/10.5194/acp-13-12003-2013>
- Oltmans, S. J., Lefohn, A. S., Shadwick, D., Harris, J. M., Scheel, H. E., Galbally, I., ... Kawasato, T. (2013). Recent tropospheric ozone changes - A pattern dominated by slow or no growth. *Atmospheric Environment*, *67*, 331–351. <https://doi.org/10.1016/j.atmosenv.2012.10.057>
- Paolini, V., Petracchini, F., Segreto, M., Tomassetti, L., Naja, N., & Cecinato, A. (2018). Environmental impact of biogas: A short review of current knowledge. *Journal of Environmental Science and Health - Part A Toxic/Hazardous Substances and Environmental Engineering*, *53*(10), 899–906. <https://doi.org/10.1080/10934529.2018.1459076>
- Sauter, F., van Zanten, M., van der Swaluw, E., Aben, J., de Leeuw, F., & van Jaarsveld, H. (2018). The OPS-model.
- Shindell, D. T., Faluvegi, G., Koch, D. M., Schmidt, G. a, Unger, N., & Bauer, S. E. (2009). Forcing to Emissions. *Interactions*, *326*(x), 716–718.
- Stensrud, D. J., Coniglio, M. C., Knopfmeier, K. H., & Clark, A. J. (2015). NUMERICAL MODELS | Model Physics Parameterization. In G. R. North, J. Pyle, & F. B. T.-E. of A. S. (Second E. Zhang (Eds.) (pp. 167–180). Oxford: Academic Press. <https://doi.org/https://doi.org/10.1016/B978-0-12-382225-3.00493-X>
- Stevens, C. J., Dupr, C., Dorland, E., Gaudnik, C., Gowing, D. J. G., Bleeker, A., ... Dise, N. B. (2010). Nitrogen deposition threatens species richness of grasslands across Europe. *Environmental Pollution*, *158*(9), 2940–2945. <https://doi.org/10.1016/j.envpol.2010.06.006>

- Stevenson, D. S., Dentener, F. J., Schultz, M. G., Ellingsen, K., van Noije, T. P. C., Wild, O., ... Szopa, S. (2006). Multimodel ensemble simulations of present-day and near-future tropospheric ozone. *Journal of Geophysical Research Atmospheres*, *111*(8). <https://doi.org/10.1029/2005JD006338>
- Tanzer, R., Malings, C., Haurlyuk, A., Subramanian, R., & Presto, A. A. (2019). Demonstration of a low-cost multi-pollutant network to quantify intra-urban spatial variations in air pollutant source impacts and to evaluate environmental justice. *International Journal of Environmental Research and Public Health*, *16*(14). <https://doi.org/10.3390/ijerph16142523>
- TNO. (2019). *Factsheet Emissies en depositie van stikstof in Nederland*. Den Haag.
- van Geffen, J. H. G. M., Eskes, H. J., Boersma, K. F., Maasackers, J. D., & Veeffkind, J. P. (2019). TROPOMI ATBD of the total and tropospheric NO₂ data products. *Royal Netherlands Meteorological Institute*. De Bilt. Retrieved from <https://sentinel.esa.int/documents/247904/2476257/Sentinel-5P-TROPOMI-ATBD-NO2-data-products>
- Velders, G. J. M., Aben, J. M. M., Geilenkirchen, G. P., den Hollander, H. A., Nguyen, L., van der Swaluw, E., ... Wichink Kruit, R. J. (2018). *Grootschalige Concentratie- en Depositiekaarten Nederland. Grootschalige Concentratie- en depositiekaarten Nederland: Rapportage 2016*. <https://doi.org/10.21945/RIVM-2018-0104>
- WHO. (2003). *Health Aspects of Air Pollution with Particulate Matter, Ozone and Nitrogen Dioxide*. <https://doi.org/10.2105/ajph.48.7.913>
- WHO. (2005). WHO Air quality guidelines for particulate matter, ozone, nitrogen dioxide and sulfur dioxide: Global update 2005, 1–21. [https://doi.org/10.1016/0004-6981\(88\)90109-6](https://doi.org/10.1016/0004-6981(88)90109-6)
- WHO. (2016). *Health and Environment: Draft road map for an enhanced global response to the adverse health effects of air pollution A69/18*. WHO.
- Williams, J. E., Boersma, K. F., Le Sager, P., & Verstraeten, W. W. (2017). The high-resolution version of TM5-MP for optimized satellite retrievals: Description and validation. *Geoscientific Model Development*, *10*(2), 721–750. <https://doi.org/10.5194/gmd-10-721-2017>
- Xiankai, L., Jiang Ming, M., & Shaofeng, D. (2008). Effects of nitrogen deposition on forest biodiversity: A review. *Shengtai Xuebao/ Acta Ecologica Sinica*, *28*(11), 5532–5548. [https://doi.org/10.1016/s1872-2032\(09\)60012-3](https://doi.org/10.1016/s1872-2032(09)60012-3)
- Xie, Y., Dai, H., Zhang, Y., Wu, Y., Hanaoka, T., & Masui, T. (2019). Comparison of health and economic impacts of PM_{2.5} and ozone pollution in China. *Environment International*, *130*(May), 104881. <https://doi.org/10.1016/j.envint.2019.05.075>
- Yasmeen, R., Li, Y., & Hafeez, M. (2019). Tracing the trade–pollution nexus in global value chains: evidence from air pollution indicators. *Environmental Science and Pollution Research*, *26*(5), 5221–5233. <https://doi.org/10.1007/s11356-018-3956-0>